

Shift current with Gaussian basis sets & general prescription for maximally-symmetric summations in the irreducible Brillouin zone

M. A. García-Blázquez,^{*,†} J. J. Esteve-Paredes,[†] A. J. Uría,[†] and J. J. Palacios^{†,‡}

[†] *Departamento de Física de la Materia Condensada, Universidad Autónoma de Madrid, E-28049 Madrid, Spain*

[‡] *Condensed Matter Physics Center (IFIMAC), Universidad Autónoma de Madrid, E-28049 Madrid, Spain*

E-mail: manuelantonio.garcia@estudiante.uam.es

Abstract

The bulk photovoltaic effect is an experimentally verified phenomenon by which a direct charge current is induced within a non-centrosymmetric material by light illumination. Calculations of its intrinsic contribution, the shift current, are nowadays amenable from first-principles employing plane-waves bases. In this work we present a general method for evaluating the shift conductivity in the framework of localized Gaussian basis sets that can be employed in both the length and velocity gauges, carrying the idiosyncrasies of the quantum-chemistry approach. The (possibly magnetic) symmetry of the system is exploited in order to fold the reciprocal space summations to the representation domain, allowing to reduce computation time and unveiling the complete symmetry properties of the conductivity tensor under general light polarization.

1 Introduction

The generation of a non-oscillating response in a material medium under an incident electric oscillating field is a general feature that occurs at all even orders in the perturbative expansion, that is, it is a non-linear optical phenomenon. For responses that transform as vectors, such as an electric current, an elementary symmetry analysis shows that all the even order response tensors must vanish in the presence of inversion symmetry, hence such frequency-independent quantity can only arise in non-centrosymmetric materials. In this regard, the emergence of a direct charge current in an homogeneous material induced by light is known as the bulk photovoltaic effect (BPVE).¹ It was established by the mid seventies with earlier experimental reports in ferroelectric materials,²⁻⁵ and continued gathering attention during the next decades.⁶⁻¹⁴ However, the potential applications in solar cells,^{15,16} and the advances in both experimental facilities and first-principles capabilities have driven a considerable surge of studies in recent years.¹⁷⁻²⁶

The BPVE is part of the total second-order optical response, which in addition includes second-harmonics and, for polychromatic electric fields, contributions of mixed frequencies. In turn, the BPVE can be separated into 3 essentially different contributions:¹⁷ the shift current, a static and coherent (stemming from the off-diagonal part of the density matrix) response that under time-reversal (\hat{T}) symmetry appears only with linearly polarized light; and two transient contributions that eventually reach a steady state, namely the injection current, which under \hat{T} symmetry appears only with circularly polarized light, and the ballistic current, which under \hat{T} symmetry emerges purely from coherent scattering processes such as electron-phonon or electron-hole interactions that introduce an imbalance between the carrier generation rates across the Brillouin zone (BZ). Disregarding excitonic effects, the BPVE in non-metallic systems occurs at frequencies above the band gap. These quantities, or equivalently the corresponding third-rank tensors $\sigma^{a;bc}(\omega)$ as a function of a single frequency, admit expressions in terms of the quasi-particle properties that are amenable to numerical evaluation via quantum mechanical methods. Specifically, these microscopic expressions can

be obtained by diagrammatic approaches for the ballistic current,^{27–29} and solving the density matrix perturbatively,¹ employing Wilson loops³⁰ or again by diagrammatic techniques³¹ for the injection and shift currents. However, only the latter one is truly intrinsic to the single-particle system, in the sense that it can be computed exclusively from the band structure and electronic eigenfunctions without further modelling.

The calculation of the shift current presents some difficulties or subtleties starting from the choice of gauge for the interaction of electrons with the field.^{31–34} The most generally applicable method, the length gauge, requires evaluating numerical derivatives with respect to the crystalline momentum \mathbf{k} of quantities that are not gauge invariant. In contrast, the velocity gauge constitutes a more straightforward alternative, although it carries an (a priori) infinite sum over the electronic states external to the direct optical transition. Both gauges require the evaluation of the matrix representation of the velocity operator in the set of crystalline eigenfunctions, and both are expected to yield equal results in the limit of a complete basis for describing the latter. There currently exist methods for evaluating the shift current in the single-particle approximation from density-functional theory (DFT),³⁵ tight-binding (including Wannierizations^{36,37}) and $\mathbf{k} \cdot \mathbf{p}$ band structures.¹⁸ Yet, as it is often the case in physics-leaning studies, the DFT calculations are almost invariably assumed to employ a plane-wave basis, at least when the velocity operator is not approximated by the momentum.

In this work, we present a formalism for computing the shift conductivity tensor in non-metallic crystals, in both length and velocity gauges, from first-principles employing Gaussian basis sets. It is based on an exact calculation of the velocity and Berry connection matrix elements through the analytical evaluation of the real-space integrals involved. The use of a localized basis presents some advantages and disadvantages with respect to the plane-waves alternative inherited from the DFT methods: the whole chain of calculations should generally be faster, the evaluation of position (and by extension, velocity) matrix elements is straightforward, hybrid functionals can be used at little cost (which may allow to obtain an

accurate gap avoiding scissor corrections or GW calculations), all-electron calculations can be performed, and no artificial replication of layers is required in 2D materials. On the other hand, a customized basis optimization has to be performed for each system while limited by the superposition error and diffusive exponents, and errors from the lack of completeness of the basis are more likely (making the more delocalized unoccupied states particularly hard to reproduce). It is expected that the reliability of this method is highly correlated with the ability to properly reproduce the relevant occupied and unoccupied states (dictated by the frequency range) with a Gaussian basis.

A further benefit of the use of localized bases lies in the guarantee that the complete symmetry of the system is preserved, in slight contrast with the maximally-localized Wannier representation. The properties of the crystallographic point group can then be exploited to reduce the summations over the BZ that are required for the shift conductivity to properly weighted sums, which encode the whole (possibly magnetic) symmetry of the system, only over its irreducible part or representation domain. We present a complete list of the explicit formulae for each space group including the magnetic configurations, where the structure type is used to parametrize the irreducible domain and the (magnetic) point group determines the precise folding of the \mathbf{k} -resolved conductivity.

2 Shift current: definition, considerations & numerical evaluation

A general expression for the total second-order optical response under homogeneous illumination can be obtained by solving the density matrix in perturbation theory for the field. In particular, for a uniform polychromatic electric field $\tilde{\mathbf{E}}(t) = \sum_j \mathbf{E}(\omega_j) e^{-i\omega_j t} + \text{c.c.}$, the shift current is defined as the intrinsic second-order DC component

$$J_{\text{shift}}^a = 2 \sum_{j | \omega_j > 0} \sum_{b,c} \text{Re} \left[\sigma_{\text{shift}}^{a;bc}(\omega_j) E^b(\omega_j) E^c(-\omega_j) \right] \quad (1)$$

where a, b, c label the spatial components in the chosen coordinate system.

2.1 Length gauge

In the length gauge, the electric potential is chosen as $\hat{V} = |e|\hat{\mathbf{r}} \cdot \mathbf{E}$ and the perturbative expression for the shift conductivity third-rank tensor in a non-metallic material ultimately reads^{14,21,38}

$$\sigma_{\text{shift}}^{a;bc}(\omega) = -\frac{ig_s\pi|e|^3}{2\hbar^2V} \sum_{\mathbf{k} \in \text{BZ}} \sum_{m,n} f_{m,n}(\mathbf{k}) [A_{m,n}^b(\mathbf{k})A_{n,m;a}^c(\mathbf{k}) - A_{n,m}^c(\mathbf{k})A_{m,n;a}^b(\mathbf{k})] \delta(\omega_{m,n}(\mathbf{k}) - \omega) \quad (2)$$

which is valid irrespective of whether time-reversal $\hat{\mathcal{T}}$ is a symmetry. In this formula

- m, n label the eigenstates of the periodic single-particle Hamiltonian $\hat{H} |\psi_{n,\mathbf{k}}\rangle = E_{n,\mathbf{k}} |\psi_{n,\mathbf{k}}\rangle$, which satisfy Bloch's theorem: $\langle \mathbf{r} | \psi_{n,\mathbf{k}} \rangle = \psi_{n,\mathbf{k}}(\mathbf{r}) = e^{i\mathbf{k}\mathbf{r}} u_{n,\mathbf{k}}(\mathbf{r})$ with $u_{n,\mathbf{k}}$ having the periodicity of the direct lattice. \mathbf{k} is the crystalline momentum or label of the irreducible representations of the translation group. $\hbar\omega_{m,n}(\mathbf{k}) \equiv E_{m,\mathbf{k}} - E_{n,\mathbf{k}}$ and $f_{m,n}(\mathbf{k}) \equiv f_m(\mathbf{k}) - f_n(\mathbf{k})$ is the difference of Fermi distributions, hereafter taken at zero temperature.
- $A_{m,n}^b(\mathbf{k}) = \langle u_{m,\mathbf{k}'} | i\hat{\partial}_{k'^b} | u_{n,\mathbf{k}'} \rangle \Big|_{\mathbf{k}}$ is the b -th spatial component of the Berry connection matrix elements, which satisfy $A_{m,n}^b(\mathbf{k}) = A_{n,m}^b(\mathbf{k})^*$.
- $A_{n,m;a}^b(\mathbf{k}) = \partial_{k'^a} A_{n,m}^b(\mathbf{k}') \Big|_{\mathbf{k}} - i[A_{n,n}^a(\mathbf{k}) - A_{m,m}^a(\mathbf{k})]A_{n,m}^b(\mathbf{k})$ is the generalized derivative (GD) of the Berry connection.
- $V = N_{\mathbf{k}} V_{\text{PUC}}$ is the volume (area in 2D, or longitude in 1D) of the crystal, with $N_{\mathbf{k}} \rightarrow \infty$ the number of terms in the Brillouin zone (BZ) summation (or discretized integration) and V_{PUC} the volume of the primitive unit cell. $\delta(\omega)$ is a nascent (or broadened) Dirac delta function. $g_s = 1$ (2) in the presence (absence, respectively) of spin-dependent terms in the Hamiltonian (excluding the doubled states in the m, n summations).

- We have introduced a global minus sign in agreement with Ref.²¹ and equation 58 of Ref.¹⁴ We note that some authors do not include the 1/2 factor in the conductivity, instead cancelling it with the prefactor in (1).

It follows that in general $\sigma_{\text{shift}}^{a;bc}(\omega) = \sigma_{\text{shift}}^{a;cb}(\omega)^* = \sigma_{\text{shift}}^{a;bc}(-\omega)^*$ and $\sigma_{\text{shift}}^{a;bb}$ is real. For linearly polarized light, $E^b(\omega_j)E^c(-\omega_j)$ is real for all components and only $\text{Re} \sigma_{\text{shift}}^{a;bc}$ contributes to J_{shift}^a . In contrast, for circular polarization $E^b(\omega_j)E^c(-\omega_j)$ is complex for some b, c , hence both the real and imaginary parts of the conductivity may contribute to the current in general. Under $\hat{\mathcal{T}}$ symmetry, in particular excluding any permanent magnetic alignment, $\hat{\mathcal{T}}u_{n,\mathbf{k}} = e^{i\theta_{n,\mathbf{k}}}u_{n,-\mathbf{k}}$ for an arbitrary phase $\theta_{n,\mathbf{k}}$; hence applying the anti-unitary transformation in the inner products, and noting that $\hat{\mathcal{T}}i\hat{\nabla}_{\mathbf{k}}\hat{\mathcal{T}}^{-1} = -i\hat{\nabla}_{\mathbf{k}}$

$$A_{m,n}^b(\mathbf{k}) = \langle u_{m,-\mathbf{k}'} | e^{-i\theta_{m,\mathbf{k}}} - i\hat{\partial}_{k^b} e^{i\theta_{n,\mathbf{k}}} | u_{n,-\mathbf{k}'} \rangle^* \Big|_{\mathbf{k}} = e^{i\theta_{n,m}^{\mathbf{k}}} \left[A_{m,n}^b(-\mathbf{k})^* + \frac{\partial \theta_{n,\mathbf{k}}}{\partial k^b} \delta_{m,n} \right] \Rightarrow$$

$$A_{n,m;a}^c(\mathbf{k}) = -e^{i\theta_{m,n}^{\mathbf{k}}} \left[\frac{\partial A_{n,m}^c(\mathbf{k}')^*}{\partial k'^a} \Big|_{-\mathbf{k}} + i (A_{n,n}^a(-\mathbf{k})^* - A_{m,m}^a(-\mathbf{k})^*) A_{n,m}^c(-\mathbf{k})^* \right] = -e^{i\theta_{m,n}^{\mathbf{k}}} A_{n,m;a}^c(-\mathbf{k})^*$$

where $\theta_{n,m}^{\mathbf{k}} \equiv \theta_{n,\mathbf{k}} - \theta_{m,\mathbf{k}}$. Thus $f_{m,n}(\mathbf{k})A_{m,n}^b(\mathbf{k})A_{n,m;a}^c(\mathbf{k}) = - [f_{m,n}(-\mathbf{k})A_{m,n}^b(-\mathbf{k})A_{n,m;a}^c(-\mathbf{k})]^*$ and $\sigma_{\text{shift}}^{a;bc}$ is real with $\hat{\mathcal{T}}$ symmetry. In this case also $-A_{n,m}^c(\mathbf{k})A_{m,n;a}^b(\mathbf{k}) = A_{m,n}^c(\mathbf{k})A_{n,m;a}^b(\mathbf{k})$ under the BZ summation. The difference between the currents for right and left circular polarization, which is proportional to $\text{Im} \sigma_{\text{shift}}^{a;bc}$ only, is therefore vanishing; and the shift current is associated with linearly polarized light. In the event of $\hat{\mathcal{T}}$ breaking, a circular shift current generally emerges as well as a non-stationary injection current.^{21,23} We remark that the injection current can be equally computed with the method described in this work, but we do not show explicit results since the calculation is straightforward compared to that for the shift current,^{14,38} up to an extrinsic scattering rate that is often set phenomenologically.

2.2 Berry connection and velocity in a local basis

The single-particle crystalline eigenstates are generally expanded in a set of states ¹ satisfying Bloch's theorem as

$$|\psi_{n,\mathbf{k}}\rangle = \sum_{\mu} c_{\mu,n}(\mathbf{k}) |\phi_{\mu,\mathbf{k}}\rangle$$

where μ is in principle a generic label and the coefficients are obtained from the generalized eigenvalue problem

$$\sum_{\mu'} [H_{\mu,\mu'}(\mathbf{k}) - E_n(\mathbf{k})S_{\mu,\mu'}(\mathbf{k})] c_{\mu',n}(\mathbf{k}) = 0$$

where the Hamiltonian $H_{\mu,\mu'}(\mathbf{k})$ and overlap $S_{\mu,\mu'}(\mathbf{k})$ matrix elements are the representations of the Hamiltonian \hat{H} and identity \hat{I} operator, respectively, in the set $\{|\phi_{\mu,\mathbf{k}}\rangle\}_{\mu}$ for each \mathbf{k} . In a local basis, which is repeated in each unit cell and labelled by the lattice vectors \mathbf{R} , the Bloch states can in turn be expanded in agreement with Bloch's theorem

$$|\phi_{\mu,\mathbf{k}}\rangle = \frac{1}{\sqrt{N}} \sum_{\mathbf{R}} e^{i\mathbf{k}\mathbf{R}} |\varphi_{\mu,\mathbf{R}}\rangle$$

where $N = V/V_{\text{PUC}} \rightarrow \infty$ is the number of unit cells in the crystal. Therefore

$$\begin{aligned} H_{\mu,\mu'}(\mathbf{k}) &= \sum_{\mathbf{R}} e^{i\mathbf{k}\mathbf{R}} H_{\mu,\mu'}(\mathbf{R}), \text{ with } H_{\mu,\mu'}(\mathbf{R}) = \langle \varphi_{\mu,\mathbf{0}} | \hat{H} | \varphi_{\mu',\mathbf{R}} \rangle, \\ S_{\mu,\mu'}(\mathbf{k}) &= \sum_{\mathbf{R}} e^{i\mathbf{k}\mathbf{R}} S_{\mu,\mu'}(\mathbf{R}), \text{ with } S_{\mu,\mu'}(\mathbf{R}) = \langle \varphi_{\mu,\mathbf{0}} | \varphi_{\mu',\mathbf{R}} \rangle \end{aligned} \quad (3)$$

due to the periodicity of $\hat{H}(\mathbf{r})$ and \hat{I} .

The Berry connection matrix elements can then be expressed in the local basis by inserting the transformation $u_{n,\mathbf{k}}(\mathbf{r}) = e^{-i\mathbf{k}\mathbf{r}} \sum_{\mu} c_{\mu,n}(\mathbf{k}) \frac{1}{\sqrt{N}} \sum_{\mathbf{R}} e^{i\mathbf{k}\mathbf{R}} \varphi_{\mu,\mathbf{R}}(\mathbf{r})$, yielding after some algebra

$$A_{m,n}^b(\mathbf{k}) = -i \left. \frac{\partial c_{\mu,m}^*(\mathbf{k}')}{\partial k'^b} \right|_{\mathbf{k}} S_{\mu,\mu'}(\mathbf{k}) c_{\mu',n}(\mathbf{k}) + c_{\mu,m}^*(\mathbf{k}) r_{\mu,\mu'}^b(\mathbf{k}) c_{\mu',n}(\mathbf{k})$$

¹Which in practice is not an actual (complete) basis in this function space due to its finiteness. Nevertheless, we use this term referring to non-complete sets according to standard convention.

which can be compactly expressed in matrix form as

$$A^b(\mathbf{k}) = -i \left. \frac{\partial c^\dagger(\mathbf{k}')}{\partial k'^b} \right|_{\mathbf{k}} S(\mathbf{k})c(\mathbf{k}) + c^\dagger(\mathbf{k})r^b(\mathbf{k})c(\mathbf{k}) \quad (4)$$

We have introduced the position matrix elements in the Bloch basis

$$\mathbf{r}_{\mu,\mu'}(\mathbf{k}) = \sum_{\mathbf{R}} e^{i\mathbf{k}\mathbf{R}} \mathbf{r}_{\mu,\mu'}(\mathbf{R}), \quad \text{with } \mathbf{r}_{\mu,\mu'}(\mathbf{R}) = \langle \varphi_{\mu,0} | \hat{\mathbf{r}} | \varphi_{\mu',\mathbf{R}} \rangle = \int_{\mathbb{R}^3} \varphi_{\mu,0}(\mathbf{r})^* \mathbf{r} \varphi_{\mu',\mathbf{R}}(\mathbf{r}) d^3\mathbf{r} \quad (5)$$

which is well defined in a localized basis, albeit the diagonal components depend on the origin choice. Indeed, a rigid shift of the form $\mathbf{r} \rightarrow \mathbf{r} + \mathbf{r}_0$ (which does not alter the position operator $\hat{\mathbf{r}}$ itself) with \mathbf{r}_0 restricted to the unit cell, results in $A_{m,n}^b(\mathbf{k}) \rightarrow A_{m,n}^b(\mathbf{k}) - \mathbf{r}_0 \delta_{m,n}$. Nevertheless, it is easy to see that this arbitrary factor is cancelled in the GD $A_{m,n;a}^b$ rendering the shift conductivity invariant under this choice.

As it can be observed in (4), the calculation of both diagonal and off-diagonal Berry connections requires evaluating numerical derivatives with respect to \mathbf{k} . In order to avoid further complications in the term $\partial_{k^a} A_{n,m}^b$ of the GD $A_{n,m;a}^b$, such as the introduction of a second grid for derivatives or the increase in the required significant digits, we employ the identity

$$\mathbf{A}_{n,m}(\mathbf{k}) = \frac{\mathbf{v}_{n,m}(\mathbf{k})}{i\omega_{n,m}(\mathbf{k})}, \quad m \neq n \quad (6)$$

which can be readily obtained by expanding $\nabla_{\mathbf{k}} \left[\langle u_{m,\mathbf{k}} | e^{-i\mathbf{k}\mathbf{r}} \hat{H} e^{i\mathbf{k}\mathbf{r}} | u_{n,\mathbf{k}} \rangle \right] = 0$ for $m \neq n$. In (6), $\mathbf{v}_{n,m}(\mathbf{k}) = \langle \psi_{n,\mathbf{k}} | \hat{\mathbf{v}} | \psi_{m,\mathbf{k}} \rangle = \mathbf{v}_{m,n}(\mathbf{k})^*$ are the matrix elements (here in the set of eigenstates) of the velocity operator $\hat{\mathbf{v}} \equiv (i/\hbar)[\hat{H}, \hat{\mathbf{r}}]$. It can be shown that the velocity matrix elements have the following form in the local basis³⁹

$$\mathbf{v}_{n,m}(\mathbf{k}) = \frac{1}{\hbar} \sum_{\mu,\mu'} c_{\mu,n}^*(\mathbf{k}) [\nabla_{\mathbf{k}} H_{\mu,\mu'}(\mathbf{k}) - E_n(\mathbf{k}) \nabla_{\mathbf{k}} S_{\mu,\mu'}(\mathbf{k}) + i\hbar\omega_{n,m}(\mathbf{k}) \mathbf{r}_{\mu,\mu'}(\mathbf{k})] c_{\mu',m}(\mathbf{k}) \quad (7)$$

which is independent on the origin choice. The \mathbf{k} -derivatives in this expression are all ana-

lytical, in particular $\nabla_{\mathbf{k}} H_{\mu,\mu'}(\mathbf{k}) = i \sum_{\mathbf{R}} e^{i\mathbf{k}\mathbf{R}} \mathbf{R} H_{\mu,\mu'}(\mathbf{R})$ and likewise for $S_{\mu,\mu'}(\mathbf{k})$. Therefore, $\partial_{k^a} A_{n,m}^b$ and $A_{n,m}^b$ can be computed employing (6) with numerical derivatives only of the first and zeroth order, respectively. Inserting these into (2), noting that the $f_{m,n}$ factor forces $m \neq n$ and that the derivatives of $\omega_{n,m}$ cancel out, one obtains

$$\begin{aligned} \sigma_{\text{shift}}^{a;bc}(\omega) &= -\frac{ig_s\pi|e|^3}{2\hbar^2V} \sum_{\mathbf{k} \in \text{BZ}} \sum_{m,n} \frac{f_{m,n}}{\omega_{m,n}^2} [v_{m,n}^b v_{n,m;a}^c - v_{n,m}^c v_{m,n;a}^b] \delta(\omega_{m,n} - \omega) = \\ &= -\frac{ig_s\pi|e|^3}{2\hbar^2V} \sum_{\mathbf{k} \in \text{BZ}} \sum_{m,n} \frac{f_{m,n}}{\omega_{m,n}^2} \left\{ v_{m,n}^b \left[\frac{\partial v_{n,m}^c}{\partial k^a} - i v_{n,m}^c (A_{n,n}^a - A_{m,m}^a) \right] - (b \leftrightarrow c)^* \right\} \delta(\omega_{m,n} - \omega) \end{aligned} \quad (8)$$

where $(b \leftrightarrow c)^*$ represents the conjugated of the previous term inside the curly brackets with the components b and c permuted (even if $b = c$), and the \mathbf{k} dependence has been omitted for brevity. Note that with $\hat{\mathcal{T}}$ symmetry the $-(b \leftrightarrow c)^*$ term is equivalent to $+(b \leftrightarrow c)$ under the BZ summation.

A subtle issue in (8) and other equivalent length gauge formulae is the evaluation of numerical derivatives of quantities that are not gauge-invariant, in particular the coefficients $c_{\mu,m}$ in the diagonal Berry connections, see (4), and the velocities $\mathbf{v}_{n,m}$ for $n \neq m$; which are respectively determined up to arbitrary phase factors $\theta_{m,\mathbf{k}}$ and $\theta_{m,n}^{\mathbf{k}} = \theta_{m,\mathbf{k}} - \theta_{n,\mathbf{k}}$. The continuity of (3) in \mathbf{k} makes all $c(\mathbf{k})$ (and $\mathbf{v}(\mathbf{k})$ by extension) also continuous, except in general for the phases. In order to fix a continuous gauge, we impose that

$$e^{i\theta_{m,\mathbf{k}}} \sum_{\mu} c_{\mu,m}(\mathbf{k}) = \left| \sum_{\mu} c_{\mu,m}(\mathbf{k}) \right| \in \mathbb{R}, \quad \forall m, \mathbf{k}$$

The necessary \mathbf{k} -derivatives are well defined this way, and the $\theta_{m,\mathbf{k}}$ factors are all cancelled in the gauge-invariant (8) by a similar argument than in the time-reversal case above. The only remaining caveat is to keep track of the correct band indexing when a degeneracy occurs between the infinitesimally close $\mathbf{k} \pm \mathbf{h}$ points defining the numerical derivatives. However, this issue may be neglected by mapping the \mathbf{k} -summation to the interior of the irreducible Brillouin zone (IBZ), where only accidental degeneracies may occur, see Section 3.

In 2D materials the out of plane tensor components, i.e., involving at least one index along the non-periodic direction \mathbf{z} , can be computed on equal footing (and likewise for 1D systems). Regarding the system as a periodic stacking of layers, $H_{\mu,\mu'}(\mathbf{R}_z)$ ², $S_{\mu,\mu'}(\mathbf{R}_z)$, $\mathbf{r}_{\mu,\mu'}(\mathbf{R}_z)$ are exponentially vanishing for inter-layer vectors \mathbf{R}_z in the limit of large layer separation, making all k^z -derivatives null. In this case (4) and (7) reduce to $A_{m,n}^z = -iv_{m,n}^z/\omega_{m,n} = \sum_{\mu,\mu'} c_{m,\mu}^\dagger r_{\mu,\mu'}^z c_{\mu',n}$. While the $a = z$ component in the shift conductivity tensor may not be of interest, in some point groups the IBZ summation requires the calculation of some of these components for $a = x, y$; in which case the numerical derivatives in (8) are cancelled and the expression is simplified significantly.

An alternative treatment of (2) that is often found in the literature^{1,14,35} consists on the introduction of the shift vector, which involves the term $\partial_{\mathbf{k}^a} \Phi_{n,m}^b(\mathbf{k})$ where $v_{n,m}^b = |v_{n,m}^b| e^{-i\Phi_{n,m}^b}$. This is obtained by noting that in the GD $\partial_{k^a} A_{n,m}^b = A_{n,m}^b \partial_{k^a} \log A_{n,m}^b$ when $A_{n,m}^b \neq 0$. The term inside the curly brackets in (8) is then equivalent to

$$-iv_{m,n}^b v_{n,m}^c \left[\frac{\partial(\Phi_{n,m}^b + \Phi_{n,m}^c)}{\partial k^a} + 2(A_{n,n}^a - A_{m,m}^a) + i \frac{\partial \log |v_{n,m}^c/v_{n,m}^b|}{\partial k^a} \right]$$

For linearly polarized light one can always rotate the coordinate system, initially based on the crystallographic structure, such that $\mathbf{E}(\omega)$ points along, say, the b direction. Then only the $\sigma^{a;bb}$ component contributes to the current along a in (1), and the computation of the tensor is slightly simplified; in particular the modulus term vanishes in the last expression. This is, however, not advisable for practical calculations because it requires evaluating the tensor for each field direction with a different coordinate system, which may also hinder the obtention of the Hamiltonian matrix elements from the electronic structure code. In this work (8) is employed instead, since the computational cost is similar.

²In charge-neutral 2D systems, the Coulomb potential may be replaced by the Parry potential instead of the usual Ewald potential in 3D.⁴⁰

2.3 Evaluation in Gaussian basis sets

The evaluation of (8) from first-principles requires thus the knowledge of the matrix elements of \hat{H} , \hat{I} and $\hat{\mathbf{r}}$ in the local basis for a sufficiently large number of lattice vectors. The first one, $H_{\mu,\mu'}(\mathbf{R})$, must be evaluated self-consistently, typically in a DFT or hybrid DFT-HF (Hartree-Fock) scheme; and is generally expected to be provided by the corresponding electronic structure code for the chosen functional. The latter two, $S_{\mu,\mu'}(\mathbf{R})$ and $\mathbf{r}_{\mu,\mu'}(\mathbf{R})$ can be manually pre-computed from the (possibly optimized) atomic structure. If the local functions are harmonic Gaussian-type orbitals (GTOs), this can be done analytically. In that case μ is a multi-index labelling the atoms a (located at \mathbf{d}_a) in the unit cell³, the pair of orbital quantum numbers l, m ($m = -l, \dots, l$), the shells λ discerning the harmonics with identical l and, in the presence of spin dependent terms in \hat{H} such as spin-orbit coupling (SOC) or magnetic ordering, the $m_s = \pm 1/2$ spin quantum number. The contracted real GTOs $\varphi_{\mu,\mathbf{R}} : \mathbb{R}^3 \rightarrow \mathbb{R}$ are then defined as^{41,42}

$$\varphi_{\mu,\mathbf{R}}(\mathbf{r}) = N_{\lambda,l} \left[\sum_j c_{l,m,j} d_{\lambda,j} G(\alpha_{\lambda,j}, \mathbf{r} - \mathbf{d}_a - \mathbf{R}) \right] X_{l,m}(\mathbf{r} - \mathbf{d}_a - \mathbf{R})$$

where $N_{\lambda,l}$ and $c_{l,m,j}$ are normalization coefficients (see Appendix E of Ref.⁴¹), $d_{\lambda,j}$ and $\alpha_{\lambda,j}$ are the selected contraction coefficients and exponents, $G(\alpha, \mathbf{r}) = e^{-\alpha r^2}$ are the Gaussian-type radial functions and $X_{l,m}(\mathbf{r})$ are the real solid harmonics. The latter are obtained from the (not normalized) spherical harmonics $Y_{l,m}(\mathbf{r})$ as

$$X_{l,m}(\mathbf{r}) = \frac{r^l}{2} \cdot \begin{cases} Y_{l,|m|}(\mathbf{r}) + Y_{l,-|m|}(\mathbf{r}), & \text{if } m \geq 0 \\ -i [Y_{l,|m|}(\mathbf{r}) - Y_{l,-|m|}(\mathbf{r})], & \text{if } m < 0 \end{cases}$$

³Ghost atoms would be treated analogously as long as they preserve the space group symmetry.

The central integrals that need be evaluated to obtain $S(\mathbf{k})$ and $\mathbf{r}(\mathbf{k})$ are then

$$I_3(\mathbf{n}, \mathbf{n}', \mathbf{r}_0, \mathbf{r}'_0, \alpha, \alpha') = I(n_x, n'_x, x_0, x'_0, \alpha, \alpha') \cdot I(n_y, n'_y, y_0, y'_0, \alpha, \alpha') \cdot I(n_z, n'_z, z_0, z'_0, \alpha, \alpha'),$$

$$I(n_x, n'_x, x_0, x'_0, \alpha, \alpha') \equiv \int_{\mathbb{R}} (x - x_0)^{n_x} (x - x'_0)^{n'_x} e^{-\alpha(x-x_0)^2 - \alpha'(x-x'_0)^2} dx = I(n_x, n'_x, x_0 - x'_0, 0, \alpha, \alpha') \quad (9)$$

The one-dimensional integrals appearing in $\mathbf{r}(\mathbf{k})$ are then computed as

$$\int_{\mathbb{R}} (x-x_0)^n (x-x'_0)^{n'} x e^{-\alpha(x-x_0)^2 - \alpha'(x-x'_0)^2} dx = x'_0 I(n_x, n'_x, x_0 - x'_0, 0, \alpha, \alpha') + I(n_x, n'_x + 1, x_0 - x'_0, 0, \alpha, \alpha')$$

There are several methods to tabulate the one-dimensional integrals in (9), e.g., by recursion over n and n' . In this work we have instead employed the following master expression, which can be deduced from Ref.⁴³

$$I(n, n', x_0, 0, \alpha, \alpha') = e^{-\tilde{\alpha} \alpha' x_0^2} x_0^{n+n'} \sqrt{\frac{\pi \tilde{\alpha}}{\alpha}} n! \sum_{k=0}^n (-1)^{n+k} \frac{(n' + k)!}{(n - k)! k!} \tilde{\alpha}^{n'+k} \sum_{h=0}^{\lfloor \frac{n'+k}{2} \rfloor} \frac{1}{(n' + k - 2h)! h!} \left(\frac{1}{4\tilde{\alpha} \alpha x_0^2} \right)^h, \quad \forall x_0 \neq 0$$

where $\tilde{\alpha} \equiv \alpha/(\alpha + \alpha')$ and

$$I(n, n', 0, 0, \alpha, \alpha') = \begin{cases} \sqrt{\frac{\pi}{2^{n+n'} (\alpha + \alpha')^{n+n'+1}}} (n + n' - 1)!!, & \text{for } n + n' \text{ even} \\ 0, & \text{for } n + n' \text{ odd} \end{cases}$$

We note that only one of $S_{\mu, \mu'}(\pm \mathbf{R})$ (and likewise for $\mathbf{r}_{\mu, \mu'}(\pm \mathbf{R})$) needs be computed for each $\mathbf{R} \neq \mathbf{0}$ since

$$S_{\mu, \mu'}(-\mathbf{R}) = S_{\mu', \mu}(\mathbf{R}), \quad \mathbf{r}_{\mu, \mu'}(-\mathbf{R}) = \mathbf{r}_{\mu', \mu}(\mathbf{R}) - \mathbf{R} S_{\mu', \mu}(\mathbf{R})$$

and only the upper or lower triangle for $\mathbf{R} = \mathbf{0}$. If needed, the number of matrix elements may be further restricted such that only atoms in the asymmetric unit are considered in, say, the

bra. The remaining entries can then be reconstructed by employing the (spinless) transformation properties of the real solid harmonics $\hat{g}^{-1}X_{l,m}(\mathbf{r}) = X_{l,m}(g\mathbf{r}) = \sum_{m'} \mathcal{D}_{m,m'}^l(g)X_{l,m'}(\mathbf{r})$, and the position operator $\hat{g}^{-1}\hat{r}^b\hat{g} = \sum_{b'} \mathcal{D}_{b,b'}^1(g)\hat{r}^{b'}$, where $g \in O(3)$ and \mathcal{D}^l is the representation of $O(3)$ of angular momentum l^{44} ($l = 1$ for \mathbf{r}). The result is

$$\begin{aligned}
S_{(\mathbf{g}a,\lambda,l,m),(\mathbf{g}'a',\lambda',l',m')}(\mathbf{R}) &= \sum_{m_1,m'_1} \mathcal{D}_{m,m_1}^l(g)^* \mathcal{D}_{m',m'_1}^{l'}(g) S_{(a,\lambda,l,m_1),(\mathbf{g}^{-1}\mathbf{g}'a',\lambda',l',m'_1)}(g^{-1}\mathbf{R}), \\
r_{(\mathbf{g}a,\lambda,l,m),(\mathbf{g}'a',\lambda',l',m')}^b(\mathbf{R}) &= \sum_{m_1,m'_1} \mathcal{D}_{m,m_1}^l(g)^* \mathcal{D}_{m',m'_1}^{l'}(g) \sum_{b'} \cdot \\
&\left[\mathcal{D}_{b,b'}^1(g) r_{(a,\lambda,l,m_1),(\mathbf{g}^{-1}\mathbf{g}'a',\lambda',l',m'_1)}^{b'}(g^{-1}\mathbf{R}) + \mathcal{D}_{b,b'}^1(g^{-1}) t^{b'} S_{(a,\lambda,l,m_1),(\mathbf{g}^{-1}\mathbf{g}'a',\lambda',l',m'_1)}(g^{-1}\mathbf{R}) \right]
\end{aligned} \tag{10}$$

where $\mathbf{g} = (g|\mathbf{t})$ is a general non-symmorphic operation in the crystallographic point group F (or space group excluding lattice translations, G/T), and $\mathbf{g}a$ represents the atom located at $\mathbf{g}\mathbf{d}_a$. Note that the atom $\mathbf{g}^{-1}\mathbf{g}'a'$ may require a non-trivial lattice vector in order to be mapped to the unit cell, thus altering $g^{-1}\mathbf{R}$. If SOC is considered, then $\hat{g}^{-1}X_{l,m,m_s}(\mathbf{r}) = \sum_{m',m'_s} \mathcal{D}_{m,m'}^l(g) \mathcal{D}_{m_s,m'_s}^{1/2}(g^{-1}) X_{l,m',m'_s}$, where $\mathcal{D}^{1/2}(c_\theta) = \mathcal{D}^{1/2}(ic_\theta) = e^{-i(\boldsymbol{\sigma}\mathbf{e})\theta/2}$ (in the $\{\uparrow, \downarrow\}$ basis order) is the projective representation of $O(3)$ of angular momentum $1/2$ which is even under inversion i ; $\boldsymbol{\sigma}$ being the Pauli vector and \mathbf{e} the counterclockwise rotation axis. The previous relations would be modified in consequence.

In plane wave schemes, $\hat{\mathbf{v}}$ is sometimes replaced by the momentum $\hat{\mathbf{p}} = -i\hbar\hat{\nabla}$. This substitution is not exact in HF or hybrid DFT-HF schemes because $\hat{\mathbf{r}}$ and the Fock operator do not commute, or likewise when employing non-local pseudopotentials or including relativistic effect such as SOC. While the deviations in the final quantities are often not large,³⁷ the increase in computational cost in the Gaussian scheme is marginal enough to advise against the use of this approximation in general, except perhaps for extremely large unit cells. Regardless, the relevant integrals would be computed as

$$\begin{aligned}
&\int_{\mathbb{R}} (x-x_0)^{n_x} e^{-\alpha(x-x_0)^2} \frac{\partial}{\partial x} (x-x'_0)^{n'_x} e^{-\alpha'(x-x'_0)^2} dx = \\
&n'_x I(n_x, n'_x - 1, x_0 - x'_0, 0, \alpha, \alpha') - 2\alpha' I(n_x, n'_x + 1, x_0 - x'_0, 0, \alpha, \alpha')
\end{aligned}$$

2.4 Velocity gauge

Alternatively, the velocity gauge can be employed by imposing the minimal coupling $\hat{H}(-i\hbar\nabla) \rightarrow \hat{H}(-i\hbar\nabla + |e|\mathcal{A})$, where \mathcal{A} is the vector potential. An analogous derivation in perturbation theory then yields^{8,23,31,33}

$$\sigma_{\text{total}}^{a;bc}(\omega) = -\frac{g_s|e|^3}{2\hbar^2\omega^2V} \sum_{\mathbf{k} \in \text{BZ}} \sum_{m,n,l} \left[\frac{f_{m,n}v_{n,m}^b}{\omega_{m,n} - \omega + i\varepsilon} \left(\frac{v_{m,l}^a v_{l,n}^c}{\omega_{m,l} + i\varepsilon} - \frac{v_{m,l}^c v_{l,n}^a}{\omega_{l,n} + i\varepsilon} \right) - (b \leftrightarrow c)^* \right]$$

Both the shift and the injection conductivities are encoded in this formula. The former can be obtained by taking only the imaginary part of the product of complex denominators in the $\varepsilon \rightarrow 0^+$ limit, which is equivalent to taking $\text{Re } \sigma_{\text{total}}^{a;bc}$ under $\hat{\mathcal{T}}$ symmetry (i.e., considering linear polarization)

$$\sigma_{\text{shift}}^{a;bc}(\omega) = \frac{g_s\pi|e|^3}{2\hbar^2V} \sum_{\mathbf{k} \in \text{BZ}} \sum_{m,n} \frac{f_{m,n}}{\omega_{m,n}^2} \text{Im} \left[v_{m,n}^b \sum_{l \neq m,n} \left(\frac{v_{n,l}^a v_{l,m}^c}{\omega_{n,l}} - \frac{v_{n,l}^c v_{l,m}^a}{\omega_{l,m}} \right) + (b \leftrightarrow c) \right] \delta(\omega_{m,n} - \omega) \quad (11)$$

In contrast with (2) and (8), the evaluation of (11) avoids the numerical derivatives at the cost of a sum over all states l that are external to the direct optical transition. Resulting from the completeness relation $\sum_n |\psi_{n,\mathbf{k}}\rangle \langle \psi_{n,\mathbf{k}}| = \hat{I}$, in principle it must span the whole set of bands (which with localized bases is seldom demanding, computationally) even if they are not well represented above a certain window from the Fermi level, but the sum should nevertheless converge to the correct result when a sufficiently large basis is employed. While the length gauge explicitly involves only the pair of bands corresponding to the direct optical transition at the field frequency, a large basis should still be needed to properly reproduce the conduction bands involved. For grids of equal size, the evaluation of (11) is more straightforward and less computationally demanding than (8), however, the assumption of completeness (which is not strictly true in finite bases) makes the length gauge approach the most reliable in general.

A similar expression to (11) that is frequently employed in the literature is obtained

within the length gauge by employing the following sum rule for the GD

$$A_{n,m;a}^b \rightarrow -\frac{1}{\omega_{n,m}} \left[(A_{n,m}^b \Delta_{n,m}^a + A_{n,m}^a \Delta_{n,m}^b) + \sum_{l \neq m,n} (v_{n,l}^b A_{l,m}^a - A_{n,l}^a v_{l,m}^b) + i w_{n,m}^{a,b} \right] \quad (12)$$

where $w_{n,m}^{a,b} \equiv \langle \psi_{n,\mathbf{k}} | [\hat{r}^a, \hat{v}^b] | \psi_{m,\mathbf{k}} \rangle = w_{n,m}^{b,a}$ and $\Delta_{n,m}(\mathbf{k}) \equiv \mathbf{v}_{n,n}(\mathbf{k}) - \mathbf{v}_{m,m}(\mathbf{k}) = \nabla_{\mathbf{k}} \omega_{n,m}(\mathbf{k})$ ⁴. This sum rule can be obtained by expanding $\partial_{k^a} \partial_{k^b} [\langle u_{m,\mathbf{k}} | e^{-i\mathbf{k}\mathbf{r}} \hat{H} e^{i\mathbf{k}\mathbf{r}} | u_{n,\mathbf{k}} \rangle] = 0$ and inserting the completeness relation above. Employing (12) in (2) yields

$$\sigma_{\text{shift}}^{a,bc}(\omega) \rightarrow -\frac{ig_s \pi |e|^3}{2\hbar^2 V} \sum_{\mathbf{k} \in \text{BZ}} \sum_{m,n} \frac{f_{m,n}}{\omega_{m,n}^2} \left\{ v_{m,n}^b \left[\sum_{l \neq m,n} \left(\frac{v_{n,l}^a v_{l,m}^c}{\omega_{n,l}} - \frac{v_{n,l}^c v_{l,m}^a}{\omega_{l,m}} \right) - \frac{v_{n,m}^a \Delta_{n,m}^c}{\omega_{n,m}} - i w_{n,m}^{a,c} \right] - (b \leftrightarrow c)^* \right\} \delta(\omega_{m,n} - \omega) \quad (13)$$

where we note that the Δ^a terms cancel out. Clearly, this expression coincides with (11) in the presence of $\hat{\mathcal{T}}$ symmetry, except for the last two terms inside the square brackets. The term $w^{a,c}$, which would clearly vanish in the absence of non-local terms in the Hamiltonian ($\hat{\mathbf{v}} = \hat{\mathbf{p}}$), is often computed in tight-binding or Wannier schemes by differentiating the Hamiltonian matrix^{18,37} but its calculation in pure DFT is non-trivial and often ignored, leaving the two-band Δ terms as the only difference in practice between the velocity gauge (11) and length gauge with sum rule (13) expressions. While the contribution of these terms is usually small, in Section 2.5 we show that the proper agreement of the length gauge formula (2) or (8) is with the velocity gauge expression (11), at least if one neglects $w^{a,c}$.

2.5 First-principles results and discussion

In Figure 1 we show the shift conductivity computed with large-sized Gaussian basis sets for some representative non-magnetic materials, in both the length (8) and velocity (11) gauges. The self-consistent electronic structure problem has been solved with the CRYSTAL code,^{45,46} from which the $H_{\mu,\mu'}(\mathbf{R})$ are readily obtained. The input files for the self-consistent

⁴The last identity results from the expansion of $\nabla_{\mathbf{k}} [\langle u_{n,\mathbf{k}} | e^{i\mathbf{k}\mathbf{r}} \hat{H} e^{i\mathbf{k}\mathbf{r}} | u_{n,\mathbf{k}} \rangle] = \nabla_{\mathbf{k}} E_{n,\mathbf{k}}$

calculations can be found in the Supporting Information, in addition to the resulting band structures.

The starting points for the basis sets were the following: in MoS₂, def2-QZVP⁴⁷ for S and pob-TZVP-rev2⁴⁸ for Mo; in GeS, def2-QZVP; in GaAs, m-pVDZ-PP-Heyd;⁴⁹ in BaTiO₃, def2-QZVP with pseudo-potential (PP) from pob-TZVP-rev2⁵⁰ for Ba. In all cases the bases were modified in order to enable (or preserve) the convergence and obtain a sufficiently accurate band structure for the conduction bands in the energy ranges displayed in Figure 1, except for GaAs which already presented a good dispersion with the unmodified Heyd basis. The standard GGA PBE functional⁵¹ was used in MoS₂, GeS and BaTiO₃ in order to facilitate contrasting with the literature, while the short-range corrected hybrid HSE06 functional⁵² was employed in GaAs for the same reason. In the latter case, the use of a hybrid functional allows to obtain the experimental band gap at Γ of ~ 1.5 eV avoiding the use of a scissor correction or a *GW* calculation.

The initial grids for the conductivity contained 2000×2000 points in the BZ for MoS₂, 1500×1500 for GeS, $400 \times 400 \times 400$ for GaAs and $200 \times 200 \times 200$ for BaTiO₃⁵; and were subsequently restricted to the IBZ as explained in Section 3, in particular employing (19) due to the absence of magnetism and the expressions from the list for the corresponding space groups: 187 (D_{3h}) reduced to 2D for MoS₂, 31 (C_{2v}) reduced to 2D with $c_{2,x}$ contained in the lattice plane for GeS, 216 (T_d) for GaAs and 99 (C_{4v}) for BaTiO₃. The delta function in the $\sigma_{\text{shift}}^{a;bc}$ expressions has been approximated by a narrow normal distribution $\delta(x) \sim \frac{1}{\sqrt{2\pi}\sigma} \exp\left[-\frac{x^2}{2\sigma^2}\right]$ with standard deviation $\sigma = 20\text{meV}$ in all cases. The absence of (unphysical) rapid fluctuations in the curves indicates that this value is not small for the chosen \mathbf{k} -grids. The numerical derivatives in the length gauge expression (8) have been symmetrized as $\partial_{k^a} f(\mathbf{k}) \sim \frac{1}{2h}(f(\mathbf{k} + h\mathbf{e}^a) - f(\mathbf{k} - h\mathbf{e}^a))$, with $h = \frac{10^{-7}}{a_0}$ in all cases. The direct lattice summations in (3) and (5) have been truncated to the first (by length) 179 vectors in MoS₂, 120 in GeS, 179 in GaAs and 260 in BaTiO₃.

⁵The grid choices were here influenced by benchmarking purposes, and substantially coarser ones will often yield good results.

The agreement with the results in the literature is generally good,^{19,23,35–37,53} specially taking into account that moderate discrepancies can be found commonly due to the high sensibility of σ_{shift} to the lattice parameters, atomic coordinates and electronic eigenfunctions,^{18,26,54} in conjunction with the different calculation methods (as outlined in the previous sections) and convergence parameters such as the BZ grid or the broadening of the delta functions. The proper description of the eigenstates in the $\hbar\omega$ energy range is critical to obtain satisfactory results, hence in principle the largest possible basis set allowed by convergence should be used, typically a reduced QZVP or augmented TZVP. Nevertheless, in materials with not particularly delocalized empty conduction states a smaller, but properly calibrated basis could suffice. It should be kept in mind that the truncation of the \mathbf{R} -sums may need to be loosed if smaller Gaussian exponents are introduced.

It can be observed in Figure 1 that the results of both length and velocity gauges are virtually identical in all cases, even if the external sum in (11) is truncated in practice by the finiteness of the basis. This is in agreement with the results of Reference³⁴ for third-order calculations in graphene. However, the inclusion of the two-band Δ terms in (13) by the sum rule induces a small, but noticeable discrepancy in some of the $\sigma_{\text{shift}}^{a;bc}$ components, specifically $\sigma^{x;yy}$, $\sigma^{y;yx}$ in GeS and $\sigma^{z;xx}$ in BaTiO₃, while all other components (including MoS₂ and GaAs) were not visibly affected. Most of the unaltered components have a symmetry reason to remain so: the Δ terms clearly do not contribute to $a = b = c$ components in (13), nor to $b = c = z$ components in 2D materials since $\Delta^z = 0$. Furthermore, it can also be seen from (13) that a sum over even permutations of (a, b, c) cancels the Δ terms, which is precisely underlying in GaAs as can be seen from the folded summation formula for T_d in Section 3. Only the $\sigma^{x;xz}$ component in BaTiO₃ cannot be explained by symmetry reasons, albeit in this case only a term of the form $v_{n,m}^z v_{m,n}^x \Delta_{n,m}^x$ contributes under $\hat{\mathcal{T}}$ symmetry, which is most likely small for numerical reasons in the dispersion along k^x .

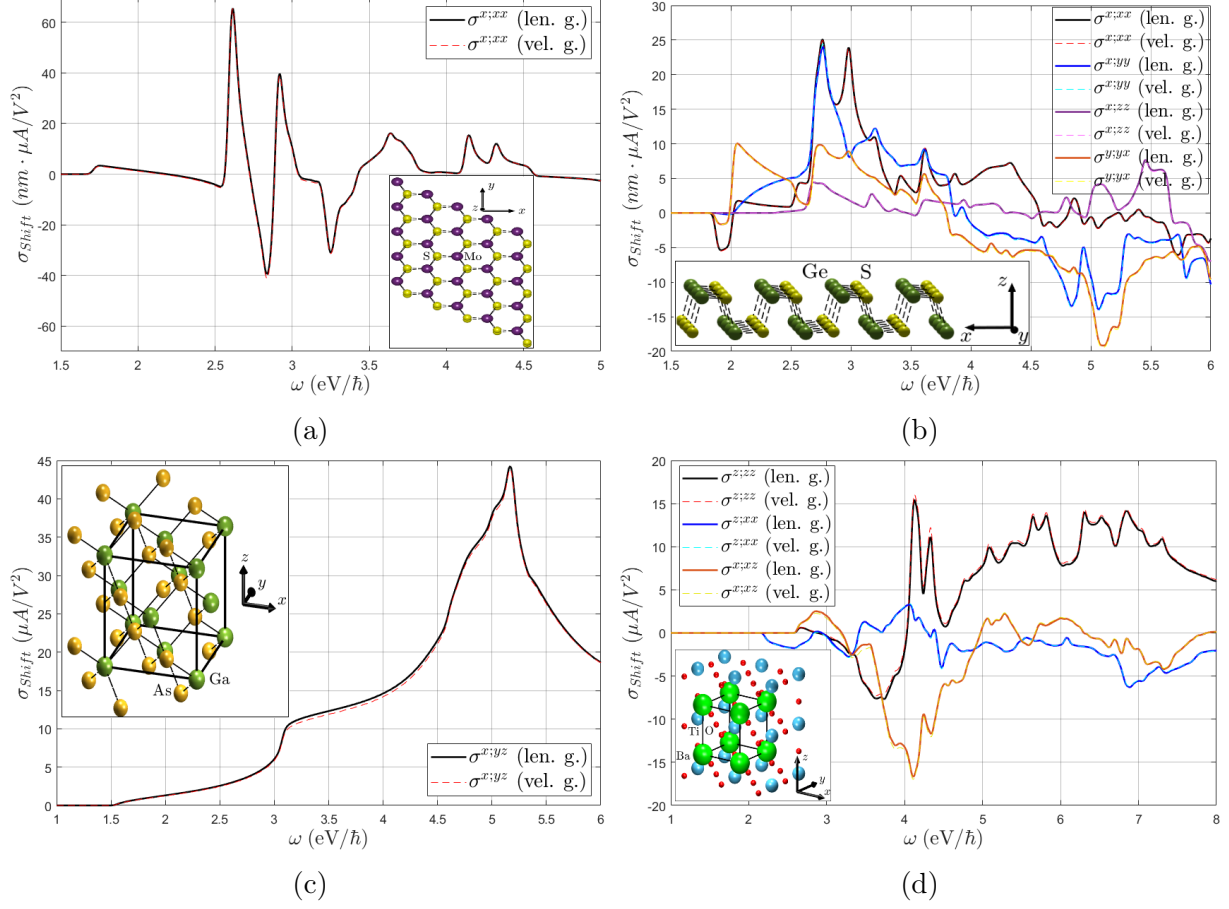


Figure 1: Shift conductivity tensor in (a) monolayer MoS₂, (b) monolayer GeS, (c) GaAs and (d) BaTiO₃ computed in the both the length (8) (solid lines) and velocity gauge (11) (dashed lines). All linearly independent components are shown in each case, excluding $\sigma^{z;zx}$ in GeS for an out of plane current. IBZ summations with time-reversal symmetry (19) have been employed.

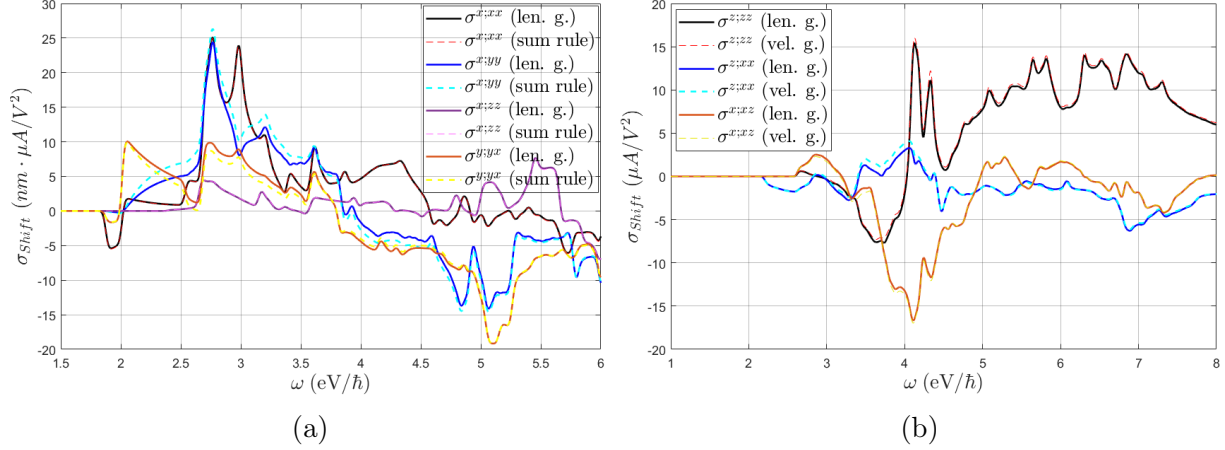


Figure 2: Shift conductivity tensor in (a) monolayer GeS and (b) BaTiO₃ computed in the length gauge (8) (solid lines) and employing the sum rule (13) (dashed lines) excluding the $w^{a,c}$ term. IBZ summations with time-reversal symmetry (19) have been employed.

3 Irreducible Brillouin Zone summation

The proper use of GTOs ensures that the crystalline eigenstates indeed transform according to the irreducible representations of the space group G , and $\hat{g}\psi_{n,\mathbf{k}}(\mathbf{r}) = \psi_{n,g\mathbf{k}}(\mathbf{r} - \mathbf{t} - \mathbf{R}) = \psi_{n,\mathbf{k}}(g^{-1}\mathbf{r})$, $\forall g = (g|\mathbf{t} + \mathbf{R}) \in G$. Then, since the velocity operator transforms under the corresponding change of coordinates as $\hat{g}^{-1}\hat{v}^b\hat{g} = \sum_{b'} \mathcal{D}_{b,b'}^1(g)\hat{v}^{b'}$ ⁶ (see discussion around (10) for context) and likewise for $\hat{\partial}_{kb}$, the following identities must be satisfied, up to an arbitrary phase factor in the eigenstates that has no impact in the conductivity

$$v_{m,n}^b(g\mathbf{k}) = \sum_{b'} \mathcal{D}_{b,b'}^1(g)v_{m,n}^{b'}(\mathbf{k}), \quad \partial_{(gk^b)} = \sum_{b'} \mathcal{D}_{b,b'}^1(g)\partial_{kb'}, \quad A_{m,n}^b(g\mathbf{k}) = \sum_{b'} \mathcal{D}_{b,b'}^1(g)A_{m,n}^{b'}(\mathbf{k}), \quad \forall g \in F \quad (14)$$

where F is the (isogonal) point group of the material, formed by disregarding all translations of the space group. On the other hand, under the time-reversal operation $\hat{\mathcal{T}}\hat{v}^b\hat{\mathcal{T}}^{-1} = -\hat{v}^b$ (odd power of time units), so that recalling from Section 2.1 the action of $\hat{\mathcal{T}}$ on the Berry

⁶Note that the translations commute with \hat{H} as fixed parameters

connection, if time-reversal is a symmetry then

$$v_{m,n}^b(-\mathbf{k}) = -v_{n,m}^b(\mathbf{k}), \quad A_{m,n}^b(-\mathbf{k}) = A_{n,m}^b(\mathbf{k}) \quad (15)$$

where again the arbitrary phase factors have been already cancelled. We note that (14), (15) hold irrespective of whether SOC is included, since the space group is the same ⁷ and the representations of the eigenstates are not being used (but rather of the operators), and the sign of $\hat{\mathcal{T}}^2 = \pm \hat{I}$ has no impact. Consequently, the following analysis is also valid irrespective of SOC.

These transformation properties can now be exploited to reduce the summations over the BZ in (2), (8) or (13) to properly weighted sums over the IBZ or representation domain, from which the whole BZ is reconstructed by applying point group symmetries (possibly including \mathcal{T}). This ensures that each sampled \mathbf{k} point provides unique information, reducing the computation time of the original BZ grid by approximately the order of the point group, and avoids the touching of symmetry-enforced degeneracies which are troublesome for computing the numerical derivatives in the length gauge. Furthermore, the identification of the finite tensor entries and the linear dependencies between them is straightforward from the IBZ expressions.

In order to avoid exceptions with duplicated points, we hereafter assume that the BZ sampling does not contain any high symmetry point (or, to be precise, any point whose little group is not trivial), which is without loss of generality in sufficiently fine grids. Several cases are distinguished depending on time-reversal symmetry, which determines the magnetic point group M .

- Magnetic point group of type I: M contains only unitary operations, i.e., $M = F$ and

⁷The space group can be regarded as unaltered if projective representations of the little groups are employed,⁴⁴ which do not appear in this derivation regardless. Alternatively, vector (standard) representations of enlarged little groups can be considered.⁵⁵ On the other hand, we disregard the extra spin-only operations of the spin-space group that may appear without SOC. These may possibly introduce further restrictions, but would not overrule the present ones in any case.

\mathcal{T} is excluded. Then by (14) the first term in (8) satisfies

$$\begin{aligned} \sum_{\mathbf{k} \in \text{IBZ}} v_{m,n}^b(\mathbf{k}) \left. \frac{\partial v_{n,m}^c(\mathbf{k}')}{\partial k'^a} \right|_{\mathbf{k}} &= \sum_{g \in F} \sum_{\mathbf{k} \in \text{IBZ}} v_{m,n}^b(g\mathbf{k}) \left. \frac{\partial v_{n,m}^c(\mathbf{k}')}{\partial k'^a} \right|_{g\mathbf{k}} = \\ &= \sum_{\mathbf{k} \in \text{IBZ}} \sum_{a',b',c'} \mathbb{D}_{a,a';b,b';c,c'}^F v_{m,n}^{b'}(\mathbf{k}) \left. \frac{\partial v_{n,m}^{c'}(\mathbf{k}')}{\partial k'^{a'}} \right|_{\mathbf{k}} \end{aligned}$$

and likewise for the other terms, also in the form of (2) or (13). Here we have defined, for any subset $L \in O(3)$,

$$\mathbb{D}_{a,a';b,b';c,c'}^L \equiv \sum_{g \in L} \mathcal{D}_{a,a'}^1(g) \mathcal{D}_{b,b'}^1(g) \mathcal{D}_{c,c'}^1(g) \quad (16)$$

Then, writing the \mathbf{k} -integrand explicitly for any of the forms (2), (8) or (13),

$$\sigma_{\text{shift}}^{a;bc} \equiv -\frac{i}{N_{\mathbf{k}}} \sum_{\mathbf{k} \in \text{BZ}} \left[\tilde{\sigma}_{\text{shift}}^{a;bc}(\mathbf{k}) - \tilde{\sigma}_{\text{shift}}^{a;cb}(\mathbf{k})^* \right] \quad (17)$$

it follows that

$$\sigma_{\text{shift}}^{a;bc} = -\frac{i}{|F|N_{\mathbf{k}}^{\text{IBZ}}} \sum_{\mathbf{k} \in \text{IBZ}} \sum_{a',b',c'} \mathbb{D}_{a,a';b,b';c,c'}^F \left[\tilde{\sigma}_{\text{shift}}^{a';b'c'}(\mathbf{k}) - \tilde{\sigma}_{\text{shift}}^{a';c'b'}(\mathbf{k})^* \right] \quad (18)$$

where we have used that $N_{\mathbf{k}} = |F|N_{\mathbf{k}}^{\text{IBZ}}$, with $|F|$ the order of F and $N_{\mathbf{k}}^{\text{IBZ}}$ the number of grid points in the IBZ. It is easy to see that $\mathbb{D}_{a,a';b,b';c,c'}^F = 0$ for any group with inversion symmetry $i \in F$, hence $\sigma_{\text{shift}}^{a;bc} = 0$ in agreement with the obvious requirement from perturbation theory.

- Magnetic point group of type II: time-reversal is a symmetry by itself, i.e., $M =$

$F + \mathcal{T}F$. This precludes any permanent magnetic ordering. Then by (14) and (15)

$$\begin{aligned} \sum_{\mathbf{k} \in \text{BZ}} v_{m,n}^b(\mathbf{k}) \left. \frac{\partial v_{n,m}^c(\mathbf{k}')}{\partial k'^a} \right|_{\mathbf{k}} &= \frac{1}{g_i} \sum_{g \in F} \sum_{\mathbf{k} \in \text{IBZ}} \left[v_{m,n}^b(g\mathbf{k}) \left. \frac{\partial v_{n,m}^c(\mathbf{k}')}{\partial k'^a} \right|_{g\mathbf{k}} + v_{m,n}^b(-g\mathbf{k}) \left. \frac{\partial v_{n,m}^c(\mathbf{k}')}{\partial k'^a} \right|_{-g\mathbf{k}} \right] = \\ & \frac{1}{g_i} \sum_{\mathbf{k} \in \text{IBZ}} \sum_{a',b',c'} \mathbb{D}_{a,a';b,b';c,c'}^F 2i \text{Im} \left[v_{m,n}^{b'}(\mathbf{k}) \left. \frac{\partial v_{n,m}^{c'}(\mathbf{k}')}{\partial k'^{a'}} \right|_{\mathbf{k}} \right] \end{aligned}$$

where $g_i = 2$ if $i \in F$ or in the 2D cases with out of plane $c_{2,z}$ rotational symmetry, and $g_i = 1$ otherwise. The group F is again forced to be non-centrosymmetric, but time-reversal symmetry effectively halves the IBZ with respect to the type I case by introducing a relation between the $\pm\mathbf{k}$ pairs (except in the cases where $g_i = 2$). The general shift current tensor (17) thus satisfies

$$\sigma_{\text{shift}}^{a;bc} = \frac{1}{|F|N_{\mathbf{k}}^{\text{IBZ}}} \sum_{\mathbf{k} \in \text{IBZ}} \sum_{a',b',c'} \mathbb{D}_{a,a';b,b';c,c'}^F \text{Im} \left[\tilde{\sigma}_{\text{shift}}^{a';b'c'}(\mathbf{k}) + \tilde{\sigma}_{\text{shift}}^{a';c'b'}(\mathbf{k}) \right] \quad (19)$$

where $N_{\mathbf{k}} = 2|F|N_{\mathbf{k}}^{\text{IBZ}}/g_i$. In agreement with Section 2.1, $\sigma_{\text{shift}}^{a;bc}$ is real in this case.

- Magnetic point group of type III: exactly half of the unitary operations are paired with time-reversal, i.e., $M = H + \mathcal{T}(F - H)$ where $H \subset F$ is an ordinary point group and $F - H$ is thus not a group. In this case (14) is valid for $g \in H$ whereas (15) must be used in combination with (14) for $g \in F - H$, and the IBZ is defined by F as in type I. Hence, symmetrizing in $\pm\mathbf{k}$,

$$\begin{aligned} \sum_{\mathbf{k} \in \text{BZ}} v_{m,n}^b(\mathbf{k}) \left. \frac{\partial v_{n,m}^c(\mathbf{k}')}{\partial k'^a} \right|_{\mathbf{k}} &= \frac{1}{2} \sum_{\mathbf{k} \in \text{IBZ}} \sum_{\mathbf{k}' = \pm\mathbf{k}} \left[\sum_{g \in H} v_{m,n}^b(g\mathbf{k}') \left. \frac{\partial v_{n,m}^c(\mathbf{k}'')}{\partial k''^a} \right|_{g\mathbf{k}'} + \right. \\ & \left. \sum_{\tilde{g} \in F-H} v_{m,n}^b(-\tilde{g}\mathbf{k}') \left. \frac{\partial v_{n,m}^c(\mathbf{k}'')}{\partial k''^a} \right|_{-\tilde{g}\mathbf{k}'} \right] = \\ & \sum_{\mathbf{k} \in \text{IBZ}} \sum_{a',b',c'} \left[\mathbb{D}_{a,a';b,b';c,c'}^H v_{m,n}^{b'}(\mathbf{k}) \left. \frac{\partial v_{n,m}^{c'}(\mathbf{k}')}{\partial k'^{a'}} \right|_{\mathbf{k}} - \mathbb{D}_{a,a';b,b';c,c'}^{F-H} v_{n,m}^{b'}(\mathbf{k}) \left. \frac{\partial v_{m,n}^{c'}(\mathbf{k}')}{\partial k'^{a'}} \right|_{\mathbf{k}} \right] \end{aligned}$$

and, noting that $\mathbb{D}^{F-H} = \mathbb{D}^F - \mathbb{D}^H$, (17) can be expressed as

$$\sigma_{\text{shift}}^{a;bc} = -\frac{i}{|F|N_{\mathbf{k}}^{\text{IBZ}}} \sum_{\mathbf{k} \in \text{IBZ}} \sum_{a',b',c'} \left[2\mathbb{D}_{a,a';b,b';c,c'}^H \text{Re} \left(\tilde{\sigma}_{\text{shift}}^{a';b'c'}(\mathbf{k}) - \tilde{\sigma}_{\text{shift}}^{a';c'b'}(\mathbf{k}) \right) - \mathbb{D}_{a,a';b,b';c,c'}^F \left(\tilde{\sigma}_{\text{shift}}^{a';b'c'}(\mathbf{k})^* - \tilde{\sigma}_{\text{shift}}^{a';c'b'}(\mathbf{k}) \right) \right] \quad (20)$$

If the crystalline structure is centrosymmetric disregarding magnetism, there are three cases upon magnetization. The first one is that i is completely removed by the magnetization, $i \notin F$ and M is of type I or III, thus it imposes no restrictions on $\sigma_{\text{shift}}^{a;bc}$. The second one is $i \in H \subset F$, which implies that $\mathbb{D}^H = \mathbb{D}^F = 0$ and $\sigma_{\text{shift}}^{a;bc} = 0$. The third one is $i \in F - H$, which implies that $\mathbb{D}^F = 0$ and $\text{Re} \sigma_{\text{shift}}^{a;bc} = 0$. Therefore, a centrosymmetric material may host a finite shift current upon magnetization as long as inversion is not a symmetry by itself but in combination with time-reversal (often termed \mathcal{PT} symmetry), a situation that is most common in antiferromagnets and which by (1) and (20) yields a shift current under circular (or elliptical) polarization.

Note that (18), (19), (20) also include the case of 2D materials with the global symmetry $\sigma_h \in F$ (mirror plane parallel to the lattice), since the required $1/2$ factor in the $\sum_{\mathbf{k} \in \text{BZ}} \rightarrow (1/2) \sum_{g \in F} \sum_{\mathbf{k} \in \text{IBZ}}$ substitution is absorbed in $|F/C_{1h}| = N_{\mathbf{k}}/N_{\mathbf{k}}^{\text{IBZ}}$.

Therefore, for a given material one must evaluate (18), (19) or (20) according to its magnetic point group, which requires computing (16) for the appropriate subgroup of $O(3)$, and parametrizing the IBZ according to its space group since the lattice type determines the BZ. In the list at the end of this section we show, for each (unitary) non-centrosymmetric point group, the values of (16) in the simplified notation $aa';bb';cc'$, excluding the vanishing components as well as those that are redundant due to the permutation properties $aa';bb';cc' = aa';cc';bb' = bb';aa';cc' = bb';cc';aa' = cc';aa';bb' = cc';bb';aa'$ and the reciprocity relation $a'a;b'b;c'c = aa';bb';cc'$. Afterwards the finite components of the $\sigma_{\text{shift}}^{a;bc}$ tensor and the relations between them are displayed, omitting the persistent $\sigma_{\text{shift}}^{a;bc} = (\sigma_{\text{shift}}^{a;cb})^*$ and

specifying which of (18) or (19) are finite if only one of them is ⁸. When multiple orientations along the Cartesian axes are possible, we indicate the orientation of the generating operations with the notation $c_{n,a}$ for a counterclockwise $2\pi/n$ -fold rotation with axis along a , σ_a for a reflection through a plane perpendicular to a and $s_{n,a}$ for the improper rotation $c_{n,a}\sigma_a$. If a different orientation is employed, then there exists a transformation $r \in O(3)$ of our coordinate system that matches the chosen orientation, and the new conductivity tensor $\bar{\sigma}^{a;bc}$ can be computed from the one given here as $\bar{\sigma}^{a;bc} = \sum_{a',b',c'} \sigma^{a';b',c'}$, which will often result in a simple permutation of coordinates.

On the other hand, the grid of the IBZ can be obtained (non-uniquely) as a restriction of a larger grid by imposing a set of linear constraints on the coefficients α_i of the $\mathbf{k} = \sum_{i=1}^{\dim} \alpha_i \mathbf{G}_i$ points (“dim” being the dimension of the lattice) in the basis of reciprocal lattice vectors \mathbf{G}_i . Specifically,

$$\text{IBZ} = \hat{R} \left\{ \sum_{i=1}^{\dim} \alpha_i \mathbf{G}_i \mid U A^t \boldsymbol{\alpha} < u \right\} \quad (21)$$

where U and u depend on the space group and are given in the list below for a particular choice of reciprocal lattice vectors $\mathbf{G}_i^{\text{ref}}$, which are those of Reference⁵⁵ (see tables 3.1 and 3.3 therein) and which we indicate in the list in 2π units for each lattice type under the first point group for which they appear. The coefficients α_i should initially be spanning the $(-1, 1)$ interval because, while a range of length 1 for each would suffice, it is not guaranteed that our specific parametrization yields the same range for each coefficient ⁹. In (21), A and R are introduced to allow for different sets of lattice vectors: A is the transformation matrix relating both sets of reciprocal vectors as

$$\begin{pmatrix} \mathbf{G}_1 \\ \vdots \\ \mathbf{G}_{\dim} \end{pmatrix} = A \begin{pmatrix} \mathbf{G}_1^{\text{ref}} \\ \vdots \\ \mathbf{G}_{\dim}^{\text{ref}} \end{pmatrix}$$

⁸For example, $\text{Im } \sigma_I^{x;y,z}$ indicates that (18) is purely imaginary and (19) is null for the $a = x, b = y, c = z$ component. Note that $\sigma_I^{a;bc} = \sigma_{II}^{a;bc}$ implies that (18) is real. We omit the mandatory equalities between (18) and (19) for $b = c$ components.

⁹Note that in this case a $N_1 \times N_2 \times N_3$ grid for the α_i coefficients corresponds to a $(N_1/2) \times (N_2/2) \times (N_3/2)$ grid of the BZ

and \hat{R} is the operator represented by the $R \in SO(\text{dim})$ rotation matrix that relates both BZs, acting on the set of \mathbf{k} points to its right. The parametrized IBZs lie within the BZ except for the triclinic and monoclinic systems. The space groups G are labelled by their international number, and the different variations of IBZs that cannot be obtained through rotations are considered.

The list can also be employed with 2D materials in the following way: first identify the 3D space group that is compatible with the two-dimensional structure, taking into account that in this case only groups with $\mathbf{G}_3^{\text{ref}} \parallel z$ and lacking non-symmorphic translations along z can be compatible. Then, if $F = C_2$ or C_{2v} , permute two columns of U to match the c_2 axis orientation¹⁰, if $F = C_s$ (σ_y) do the columns permutation (123) \rightarrow (132), if $F = C_s$ (σ_x) do the columns permutation (123) \rightarrow (231); and if any of these 3 permutations was performed, do the same permutation of the (x, y, z) indices in aa' ; bb' ; cc' and $\sigma^{a;bc}$. Finally, eliminate all rows in U and u whose first two entries in U are zero. The reduction of IBZs with $\hat{\mathcal{T}}$ has been chosen such that the last step yields the correct IBZ in 2D (invariant with $c_{2,z}$ or halved without it) with all compatible space groups.

Either the red or the blue rows in U and u are included for a given system, in particular the red rows (excluding the blue) are included when the IBZ is not affected by \mathcal{T} , and the blue rows (excluding the red) when the IBZ is halved by \mathcal{T} . This can be determined for the 4 types of magnetic space groups,⁵⁵ which we denote as MG , as an application of the previous discussion of magnetic point groups, in addition to the specific formula for $\sigma_{\text{shift}}^{a;bc}$.

- Magnetic space group of type I: $MG = G \rightarrow$ red rows, equation (18).
- Magnetic space group of type II: $MG = G + \mathcal{T}G \rightarrow$ blue rows, equation (19).
- Magnetic space group of type III: $MG = \tilde{G} + \mathcal{T}(G - \tilde{G})$, where \tilde{G} is a space group whose point group has half the order of G 's point group, the latter of which determines the IBZ \rightarrow red rows, equation (20).

¹⁰For example, in the GeS C_{2v} (c_{2x}) geometry of the present work, the first and third columns are permuted.

- Magnetic space group of type IV: $MG = G + \mathcal{T}(e|\mathbf{t}_0)G$, where $(e|\mathbf{t}_0) \notin G$ is a pure translation. The IBZ is defined by G , for our purpose with \mathcal{T} since the extra translation, as in non-symmorphic groups, is inconsequential \rightarrow blue rows, equation (19).

- $F = C_1$

$$aa'; bb'; cc' = \delta_{a,a'}\delta_{b,b'}\delta_{c,c'}$$

No restrictions on $\sigma^{a;bc}$

- $G = 1 [\Gamma_t]$

$$\mathbf{G}_i \text{ arbitrary, } (A = R = I), U = \begin{pmatrix} -1 & 0 & 0 \\ \mathbf{1} & \mathbf{0} & \mathbf{0} \\ \mathbf{1} & \mathbf{0} & \mathbf{0} \\ 0 & -1 & 0 \\ 0 & 1 & 0 \\ 0 & 0 & -1 \\ 0 & 0 & 1 \end{pmatrix}, u = \begin{pmatrix} 0 \\ \mathbf{1} \\ \mathbf{1/2} \\ 0 \\ 1 \\ 0 \\ 1 \end{pmatrix}$$

- $F = C_2 (c_{2,z})$

$$zz; zz; zz = 2, zz; xx; xx = 2, zz; yy; yy = 2, xx; yy; zz = 2$$

$$\sigma^{z;zz}, \sigma^{z;xx}, \sigma^{z;yy}, \sigma^{x;xz}, \sigma^{y;yz}, \sigma^{x;yz}, \sigma^{y;zx}, \sigma^{z;xy}$$

- $G = 3 - 4 [\Gamma_m]$

$$\begin{pmatrix} \mathbf{G}_1^{\text{ref}} \\ \mathbf{G}_2^{\text{ref}} \\ \mathbf{G}_3^{\text{ref}} \end{pmatrix} = \begin{pmatrix} -1/(b \cdot \tan \gamma) & -1/b & 0 \\ 1/(a \cdot \sin \gamma) & 0 & 0 \\ 0 & 0 & 1/c \end{pmatrix}, U = \begin{pmatrix} -1 & 0 & 0 \\ \mathbf{1} & \mathbf{0} & \mathbf{0} \\ 0 & -1 & 0 \\ 0 & 1 & 0 \\ 0 & 0 & -1 \\ \mathbf{0} & \mathbf{0} & \mathbf{1} \\ \mathbf{0} & \mathbf{0} & \mathbf{1} \end{pmatrix}, u = \begin{pmatrix} 0 \\ \mathbf{1/2} \\ 0 \\ 1 \\ 0 \\ \mathbf{1/2} \\ \mathbf{1} \end{pmatrix}$$

◦ $G = 5 [\Gamma_m^b]$

$$\begin{pmatrix} \mathbf{G}_1^{\text{ref}} \\ \mathbf{G}_2^{\text{ref}} \\ \mathbf{G}_3^{\text{ref}} \end{pmatrix} = \begin{pmatrix} -1/(b \cdot \tan \gamma) & -1/b & 0 \\ 1/(a \cdot \sin \gamma) & 0 & -1/c \\ 1/(a \cdot \sin \gamma) & 0 & 1/c \end{pmatrix}, \quad U, u \text{ as in } G = 3$$

• $F = C_s (\sigma_z)$

$$xx; xx; xx = 2, \quad yy; yy; yy = 2, \quad xx; yy; yy = 2, \quad yy; xx; xx = 2, \quad xx; zz; zz = 2, \quad yy; zz; zz = 2$$

$$\sigma^{x;xx}, \sigma^{y;yy}, \sigma^{x;yy}, \sigma^{y;xx}, \sigma^{x;xy}, \sigma^{y;yx}, \sigma^{x;zz}, \sigma^{y;zz}, \sigma^{z;zx}, \sigma^{z;zy}$$

◦ $G = 6 - 7 [\Gamma_m]$

$$U = \begin{pmatrix} -1 & 0 & 0 \\ 1 & 0 & 0 \\ 1 & 0 & 0 \\ 0 & -1 & 0 \\ 0 & 1 & 0 \\ 0 & 0 & -1 \\ 0 & 0 & 1 \end{pmatrix}, \quad u = \begin{pmatrix} 0 \\ 1/2 \\ 1 \\ 0 \\ 1 \\ 0 \\ 1/2 \end{pmatrix}$$

◦ $G = 8 - 9 [\Gamma_m^b]$

U, u as in $G = 6$

• $F = D_2$

$$xx; yy; zz = 4$$

$$\sigma^{x;yz}, \sigma^{y;zx}, \sigma^{z;xy}$$

◦ $G = 16 - 19 [\Gamma_o]$

$$\begin{pmatrix} \mathbf{G}_1^{\text{ref}} \\ \mathbf{G}_2^{\text{ref}} \\ \mathbf{G}_3^{\text{ref}} \end{pmatrix} = \begin{pmatrix} 0 & -1/b & 0 \\ 1/a & 0 & 0 \\ 0 & 0 & 1/c \end{pmatrix}, \quad U = \begin{pmatrix} 1 & 0 & 0 \\ -1 & 0 & 0 \\ 0 & -1 & 0 \\ 0 & 1 & 0 \\ 0 & 0 & -1 \\ 0 & 0 & 1 \\ 0 & 0 & -1 \end{pmatrix}, \quad u = \begin{pmatrix} 0 \\ 1/2 \\ 0 \\ 1/2 \\ 0 \\ 1/2 \\ 1/2 \end{pmatrix}$$

◦ $G = 20 - 21 [\Gamma_o^b]$. $\eta \equiv \frac{b^2 - a^2}{b^2 + a^2}$

$$\begin{pmatrix} \mathbf{G}_1^{\text{ref}} \\ \mathbf{G}_2^{\text{ref}} \\ \mathbf{G}_3^{\text{ref}} \end{pmatrix} = \begin{pmatrix} 1/a & -1/b & 0 \\ 1/a & 1/b & 0 \\ 0 & 0 & 1/c \end{pmatrix} \text{ with } a > b, U = \begin{pmatrix} 1 & 1 & 0 \\ \eta & 1 & 0 \\ 0 & 0 & 1 \\ 1 & -1 & 0 \\ -1 & -1 & 0 \\ 0 & 0 & -1 \\ 0 & 0 & -1 \end{pmatrix}, u = \begin{pmatrix} 1 \\ 1/2 \\ 1/2 \\ 0 \\ 0 \\ 0 \\ 1/2 \end{pmatrix}$$

◦ $G = 22 [\Gamma_o^f]$

$$\begin{pmatrix} \mathbf{G}_1^{\text{ref}} \\ \mathbf{G}_2^{\text{ref}} \\ \mathbf{G}_3^{\text{ref}} \end{pmatrix} = \begin{pmatrix} 1/a & 1/b & 1/c \\ -1/a & -1/b & 1/c \\ 1/a & -1/b & -1/c \end{pmatrix}$$

* Variation 1: $a^{-2} \geq b^{-2} + c^{-2}$. $\mu_{ab} \equiv \frac{-a^2b^2 + a^2c^2 + b^2c^2}{a^2b^2 + a^2c^2 + b^2c^2}$, $\mu_{ac} \equiv \frac{a^2b^2 - a^2c^2 + b^2c^2}{a^2b^2 + a^2c^2 + b^2c^2}$

$$U = \begin{pmatrix} 1 & -\mu_{ab} & \mu_{ab} + \mu_{ac} - 1 \\ 1 & -1 & -1 \\ 1 & 1 & -1 \\ -1 & 1 & 1 \\ -1 & 1 & -1 \\ -1 & -1 & 1 \\ -1 & -1 & 1 \\ \mu_{ab} & -1 & \mu_{ac} \end{pmatrix}, u = \begin{pmatrix} 1/2 \\ 1 \\ 1 \\ 0 \\ 0 \\ 0 \\ 1 \\ 1/2 \end{pmatrix}$$

* Variation 2: $a^{-2} < b^{-2} + c^{-2}$ and $b^{-2} < c^{-2} + a^{-2}$. $\mu_{ab} \equiv \frac{-a^2b^2 + a^2c^2 + b^2c^2}{a^2b^2 + a^2c^2 + b^2c^2}$,

$$\mu_{ac} \equiv \frac{a^2b^2 - a^2c^2 + b^2c^2}{a^2b^2 + a^2c^2 + b^2c^2}$$

$$U = \begin{pmatrix} 1 & -\mu_{ab} & \mu_{ab} + \mu_{ac} - 1 \\ 1 & -1 & -1 \\ 1 & 1 & -1 \\ 1 & -1 & 1 \\ -1 & 1 & 1 \\ -1 & 1 & -1 \\ -1 & -1 & 1 \\ -1 & -1 & 1 \\ \mu_{ab} & -1 & \mu_{ac} \end{pmatrix}, u = \begin{pmatrix} 1/2 \\ 1 \\ 1 \\ 1 \\ 0 \\ 0 \\ 0 \\ 1 \\ 1/2 \end{pmatrix}$$

◦ $G = 23 - 24 [\Gamma_o^v]$. $\eta_{ab} \equiv \frac{a^2}{a^2+b^2}$, $\eta_{ac} \equiv \frac{a^2}{a^2+c^2}$, $\eta_{bc} \equiv \frac{b^2}{b^2+c^2}$

$$\begin{pmatrix} \mathbf{G}_1^{\text{ref}} \\ \mathbf{G}_2^{\text{ref}} \\ \mathbf{G}_3^{\text{ref}} \end{pmatrix} = \begin{pmatrix} 1/a & 0 & 1/c \\ 0 & -1/b & 1/c \\ 1/a & -1/b & 0 \end{pmatrix} \text{ with } c = \max(a, b, c),$$

$$U = \begin{pmatrix} 1 & \eta_{ac} & 1 - \eta_{ac} \\ \eta_{bc} & 2\eta_{bc} - 1 & \eta_{bc} - 1 \\ 1 - \eta_{ab} & -\eta_{ab} & 1 - 2\eta_{ab} \\ 1 & 1 & 0 \\ 0 & 1 & 1 \\ -1 & 0 & -1 \\ -1 & -1 & 0 \\ -1 & -1 & 0 \\ 1 - 2\eta_{ac} & -\eta_{ac} & 1 - \eta_{ac} \\ -\eta_{bc} & -1 & \eta_{bc} - 1 \end{pmatrix}, \quad u = \begin{pmatrix} 1/2 \\ 1/2 \\ 1/2 \\ 1 \\ 0 \\ 0 \\ 0 \\ 1 \\ 1/2 \\ 1/2 \end{pmatrix}$$

• $F = C_{2v} (c_{2,z}, \sigma_x)$

$$zz; zz; zz = 4, \quad zz; xx; xx = 4, \quad zz; yy; yy = 4$$

$$\sigma^{z;zz}, \sigma^{z;xx}, \sigma^{z;yy}, \sigma^{x;xz}, \sigma^{y;yz}$$

◦ $G = 25 - 34 [\Gamma_o]$ → Same as $G = 16$

◦ $G = 35 - 41 [\Gamma_o^b]$ → Same as $G = 20$

◦ $G = 42 - 43 [\Gamma_o^f]$ → Same as $G = 22$

◦ $G = 44 - 46 [\Gamma_o^v]$ → Same as $G = 23$

• $F = C_4 (c_{4,z})$

$$zz; zz; zz = 4, \quad zz; xx; xx = zz; yy; yy = zz; xy; xy = 2, \quad xx; yy; zz = -xy; yx; zz = 2$$

$$\sigma^{z;zz}, \sigma^{z;xx} = \sigma^{z;yy}, \quad \sigma^{x;xz} = \sigma^{y;yz}, \quad \sigma^{x;yz} = -\sigma^{y;zx}, \quad \text{Im } \sigma_I^{z;xy}$$

◦ $G = 75 - 78 [\Gamma_q]$

$$\begin{pmatrix} \mathbf{G}_1^{\text{ref}} \\ \mathbf{G}_2^{\text{ref}} \\ \mathbf{G}_3^{\text{ref}} \end{pmatrix} = \begin{pmatrix} 1/a & 0 & 0 \\ 0 & 1/a & 0 \\ 0 & 0 & 1/c \end{pmatrix}, U = \begin{pmatrix} -1 & 0 & 0 \\ 1 & 0 & 0 \\ 0 & -1 & 0 \\ 0 & 1 & 0 \\ 0 & 0 & 1 \\ 0 & 0 & -1 \\ 0 & 0 & -1 \end{pmatrix}, u = \begin{pmatrix} 0 \\ 1/2 \\ 0 \\ 1/2 \\ 1/2 \\ 0 \\ 1/2 \end{pmatrix}$$

◦ $G = 79 - 80 [\Gamma_v^v]$

$$\begin{pmatrix} \mathbf{G}_1^{\text{ref}} \\ \mathbf{G}_2^{\text{ref}} \\ \mathbf{G}_3^{\text{ref}} \end{pmatrix} = \begin{pmatrix} 0 & 1/a & 1/c \\ 1/a & 0 & 1/c \\ 1/a & 1/a & 0 \end{pmatrix}$$

* Variation 1: $a > c$. $\eta_{ac} \equiv \frac{a^2}{a^2+c^2}$

$$U = \begin{pmatrix} \eta_{ac} & 1 & 1 - \eta_{ac} \\ 1 & 1 & 2 \\ -1 & 0 & -1 \\ 0 & -1 & -1 \\ 1 & \eta_{ac} & 1 - \eta_{ac} \\ -1 & -1 & 0 \\ -\eta_{ac} & 1 - 2\eta_{ac} & 1 - \eta_{ac} \\ 1 - 2\eta_{ac} & -\eta_{ac} & 1 - \eta_{ac} \end{pmatrix}, u = \begin{pmatrix} 1/2 \\ 1 \\ 0 \\ 0 \\ 1/2 \\ 0 \\ 1/2 \\ 1/2 \end{pmatrix}$$

* Variation 2: $c > a$. $\eta_{ac} \equiv \frac{a^2}{a^2+c^2}$

$$U = \begin{pmatrix} \eta_{ac} & 1 & 1 - \eta_{ac} \\ 1 & 1 & 2 \\ 1 & 1 & 0 \\ -1 & 0 & -1 \\ 0 & -1 & -1 \\ 1 & \eta_{ac} & 1 - \eta_{ac} \\ -1 & -1 & 0 \\ -1 & -1 & 0 \\ -\eta_{ac} & 1 - 2\eta_{ac} & 1 - \eta_{ac} \\ 1 - 2\eta_{ac} & -\eta_{ac} & 1 - \eta_{ac} \end{pmatrix}, u = \begin{pmatrix} 1/2 \\ 1 \\ 1 \\ 0 \\ 0 \\ 1/2 \\ 0 \\ 1 \\ 1/2 \\ 1/2 \end{pmatrix}$$

- $F = S_4 (s_{4,z})$

$$zz; xx; xx = zz; yy; yy = -zz; xy; xy = 2, \quad xx; yy; zz = xy; yx; zz = 2$$

$$\sigma^{z;xx} = -\sigma^{z;yy}, \quad \sigma^{x;xz} = -\sigma^{y;yz}, \quad \sigma^{x;yz} = \sigma^{y;zx}, \quad \sigma_I^{z;xy} = \sigma_{II}^{z;xy}$$

- $G = 81 [\Gamma_q] \rightarrow$ Same as $G = 75$

- $G = 82 [\Gamma_q^v] \rightarrow$ Same as $G = 79$

- $F = D_4 (c_{4,z}, c_{2,x})$

$$xx; yy; zz = -xy; yx; zz = 4,$$

$$\sigma^{x;yz} = -\sigma^{y;zx}, \quad \text{Im } \sigma_I^{z;xy}$$

- $G = 89 - 96 [\Gamma_q]$

$$U = \begin{pmatrix} 1 & -1 & 0 \\ -1 & 0 & 0 \\ 0 & 0 & -1 \\ 0 & 0 & 1 \\ 0 & 1 & 0 \\ 0 & 0 & -1 \end{pmatrix}, \quad u = \begin{pmatrix} 0 \\ 0 \\ 0 \\ 1/2 \\ 1/2 \\ 1/2 \end{pmatrix}$$

- $G = 97 - 98 [\Gamma_q^v]$

* Variation 1: $a > c$. $\eta_{ac} \equiv \frac{a^2}{a^2+c^2}$

$$U = \begin{pmatrix} \eta_{ac} & 1 & 1 - \eta_{ac} \\ 1 & 1 & 2 \\ 1 & -1 & 0 \\ -1 & 0 & -1 \\ -1 & -1 & 0 \\ -\eta_{ac} & 1 - 2\eta_{ac} & 1 - \eta_{ac} \end{pmatrix}, \quad u = \begin{pmatrix} 1/2 \\ 1 \\ 0 \\ 0 \\ 0 \\ 1/2 \end{pmatrix}$$

* Variation 2: $c > a$. $\eta_{ac} \equiv \frac{a^2}{a^2+c^2}$

$$U = \begin{pmatrix} \eta_{ac} & 1 & 1 - \eta_{ac} \\ 1 & 1 & 2 \\ 1 & 1 & 0 \\ 1 & -1 & 0 \\ -1 & 0 & -1 \\ -1 & -1 & 0 \\ -\eta_{ac} & 1 - 2\eta_{ac} & 1 - \eta_{ac} \\ -1 & -1 & 0 \end{pmatrix}, u = \begin{pmatrix} 1/2 \\ 1 \\ 1 \\ 0 \\ 0 \\ 0 \\ 1/2 \\ 1 \end{pmatrix}$$

- $F = C_{4v} (c_{4,z}, \sigma_x)$

$$zz; zz; zz = 8, zz; xx; xx = zz; yy; yy = zz; xy; xy = 4$$

$$\sigma^{z;zz}, \sigma^{z;xx} = \sigma^{z;yy}, \sigma^{x;xz} = \sigma^{y;yz}$$

- $G = 99 - 106 [\Gamma_q] \rightarrow$ Same as $G = 89$

- $G = 107 - 110 [\Gamma_q^v] \rightarrow$ Same as $G = 97$

- $F = D_{2d} (s_{4,z}, c_{2,x})$

$$xx; yy; zz = xy; yx; zz = 4,$$

$$\sigma^{x;yz} = \sigma^{y;zx}, \sigma_I^{z;xy} = \sigma_{II}^{z;xy}$$

- $G = 111 - 118 [\Gamma_q] \rightarrow$ Same as $G = 89$

- $G = 119 - 122 [\Gamma_q^v] \rightarrow$ Same as $G = 97$

- $F = C_3 (c_{3,z})$

$$xx; xx; xx = -xx; xy; xy = 3/4, yy; yy; yy = -yy; yx; yx = 3/4, zz; zz; zz = 3,$$

$$zz; xx; xx = zz; yy; yy = zz; xy; xy = 3/2, xx; yy; zz = -xy; yx; zz = 3/2$$

$$\sigma^{x;xx} = -\sigma^{x;yy} = -\sigma_I^{y;yx} = -\sigma_{II}^{y;yx}, \quad \sigma^{y;yy} = -\sigma^{y;xx} = -\sigma_I^{x;xy} = -\sigma_{II}^{x;xy}, \quad \sigma^{z;zz}, \quad \sigma^{z;xx} = \sigma^{z;yy},$$

$$\sigma^{x;xz} = \sigma^{y;yz}, \quad \sigma^{x;yz} = -\sigma^{y;zx}, \quad \text{Im } \sigma_I^{z;xy}$$

$$\circ G = 143 - 145 [\Gamma_h]$$

$$\begin{pmatrix} \mathbf{G}_1^{\text{ref}} \\ \mathbf{G}_2^{\text{ref}} \\ \mathbf{G}_3^{\text{ref}} \end{pmatrix} = \begin{pmatrix} 1/\sqrt{3}a & -1/a & 0 \\ 2/\sqrt{3}a & 0 & 0 \\ 0 & 0 & 1/c \end{pmatrix}, \quad U = \begin{pmatrix} 1 & 0 & 0 \\ 0 & 0 & -1 \\ 0 & 0 & 1 \\ 1 & 2 & 0 \\ -1 & 1 & 0 \\ -1 & -1 & 0 \\ 0 & -1 & 0 \\ -2 & -1 & 0 \end{pmatrix}, \quad u = \begin{pmatrix} 0 \\ 1/2 \\ 1/2 \\ 1 \\ 1 \\ 0 \\ 0 \\ 1 \end{pmatrix}$$

$$\circ G = 146 [\Gamma_{rh}]$$

$$\begin{pmatrix} \mathbf{G}_1^{\text{ref}} \\ \mathbf{G}_2^{\text{ref}} \\ \mathbf{G}_3^{\text{ref}} \end{pmatrix} = \begin{pmatrix} 0 & -2/3a & 1/3c \\ 1/\sqrt{3}a & 1/3a & 1/3c \\ -1/\sqrt{3}a & 1/3a & 1/3c \end{pmatrix}$$

$$* \text{ Variation 1: } a > \sqrt{2}c. \quad \eta_{ac} \equiv \frac{a^2-2c^2}{a^2+c^2}, \quad \eta_{a4c} \equiv \frac{2a^2-4c^2}{a^2+4c^2}$$

$$U = \begin{pmatrix} \eta_{a4c} & 2 & \eta_{a4c} \\ 0 & 1 & -1 \\ -\eta_{a4c} & -\eta_{a4c} & -2 \\ -1 & 0 & 1 \\ 1 & -1 & 0 \\ -2 & -\eta_{a4c} & -\eta_{a4c} \\ -1 & 1 & 0 \\ 0 & -1 & 1 \end{pmatrix}, \quad u = \begin{pmatrix} 1 \\ 1 \\ 1 \\ 0 \\ 0 \\ 1 \\ 1 \\ 0 \end{pmatrix}$$

* Variation 2: $a < \sqrt{2}c$. $\eta_{ac} \equiv \frac{a^2-2c^2}{a^2+c^2}$, $\eta_{a4c} \equiv \frac{2a^2-4c^2}{a^2+4c^2}$

$$U = \begin{pmatrix} \eta_{a4c} & 2 & \eta_{a4c} \\ 1 & 1 & \eta_{ac} \\ -\eta_{a4c} & -\eta_{a4c} & -2 \\ -1 & 0 & 1 \\ 1 & 1 & 1 \\ 1 & -1 & 0 \\ \eta_{ac} & 1 & 1 \\ -2 & -\eta_{a4c} & -\eta_{a4c} \\ 0 & -1 & 1 \\ -1 & -1 & -1 \\ -1 & -\eta_{ac} & -1 \end{pmatrix}, u = \begin{pmatrix} 1 \\ 1 \\ 1 \\ 0 \\ 3/2 \\ 0 \\ 1 \\ 1 \\ 0 \\ 3/2 \\ 1 \end{pmatrix}$$

• $F = D_3 (c_{3,z}, c_{2,x})$

$$xx; xx; xx = -xx; xy; xy = 3/2, \quad xx; yy; zz = -xy; yx; zz = 3$$

$$\sigma^{x;xx} = -\sigma^{x;yy} = -\sigma_I^{y;yx} = -\sigma_{II}^{y;yx}, \quad \sigma^{x;yz} = -\sigma^{y;zx}, \quad \text{Im } \sigma_I^{z;xy}$$

◦ $G = 149 - 154 [\Gamma_h]$

$$U = \begin{pmatrix} 1 & 0 & 0 \\ 0 & 0 & -1 \\ 0 & 0 & 1 \\ 1 & 2 & 0 \\ -2 & -1 & 0 \\ -1 & 1 & 0 \\ -1 & -1 & 0 \end{pmatrix}, u = \begin{pmatrix} 0 \\ 1/2 \\ 1/2 \\ 1 \\ 0 \\ 1 \\ 0 \end{pmatrix}$$

◦ $G = 155 [\Gamma_{rh}]$

* Variation 1: $a > \sqrt{2}c$. $\eta_{ac} \equiv \frac{a^2-2c^2}{a^2+c^2}$, $\eta_{a4c} \equiv \frac{2a^2-4c^2}{a^2+4c^2}$

$$U = \begin{pmatrix} \eta_{a4c} & 2 & \eta_{a4c} \\ 0 & 1 & -1 \\ -\eta_{a4c} & -\eta_{a4c} & -2 \\ -1 & 0 & 1 \\ 1 & -1 & 0 \\ -1 & -1 & -1 \end{pmatrix}, u = \begin{pmatrix} 1 \\ 1 \\ 1 \\ 0 \\ 0 \\ 0 \end{pmatrix}$$

* Variation 2: $a < \sqrt{2}c$. $\eta_{ac} \equiv \frac{a^2-2c^2}{a^2+c^2}$, $\eta_{a4c} \equiv \frac{2a^2-4c^2}{a^2+4c^2}$

$$U = \begin{pmatrix} \eta_{a4c} & 2 & \eta_{a4c} \\ 1 & 1 & \eta_{ac} \\ -\eta_{a4c} & -\eta_{a4c} & -2 \\ -1 & 0 & 1 \\ 1 & 1 & 1 \\ 1 & -1 & 0 \\ -1 & -1 & -1 \\ -1 & -\eta_{ac} & -1 \\ -1 & -1 & -1 \end{pmatrix}, u = \begin{pmatrix} 1 \\ 1 \\ 1 \\ 0 \\ 3/2 \\ 0 \\ 3/2 \\ 1 \\ 0 \end{pmatrix}$$

• $F = C_{3v} (c_{3,z}, \sigma_y)$

$$xx; xx; xx = -xx; xy; xy = 3/2, zz; zz; zz = 6, zz; xx; xx = zz; yy; yy = zz; xy; xy = 3$$

$$\sigma^{x;xx} = -\sigma^{x;yy} = -\sigma_I^{y;yx} = -\sigma_{II}^{y;yx}, \sigma^{z;zz}, \sigma^{z;xx} = \sigma^{z;yy}, \sigma^{x;xz} = \sigma^{y;yz}$$

◦ $G = 156 - 159 [\Gamma_h] \rightarrow$ Same as $G = 149$

◦ $G = 160 - 161 [\Gamma_{rh}] \rightarrow$ Same as $G = 155$

• $F = C_6 (c_{6,z})$

$$zz; zz; zz = 6, zz; xx; xx = zz; yy; yy = zz; xy; xy = 3, xx; yy; zz = -xy; yx; zz = 3$$

$$\sigma^{z;zz}, \sigma^{z;xx} = \sigma^{z;yy}, \sigma^{x;xz} = \sigma^{y;yz}, \sigma^{x;yz} = -\sigma^{y;zx}, \text{Im } \sigma^{z;xy}$$

◦ $G = 168 - 173 [\Gamma_h]$

$$U = \begin{pmatrix} 1 & 0 & 0 \\ 0 & 0 & 1 \\ 0 & 0 & -1 \\ 0 & 0 & -1 \\ 1 & 2 & 0 \\ -1 & 1 & 0 \\ -1 & -1 & 0 \end{pmatrix}, u = \begin{pmatrix} 0 \\ 1/2 \\ 0 \\ 1/2 \\ 1 \\ 1 \\ 0 \end{pmatrix}$$

- $F = C_{3h} (c_{3,z}, \sigma_z)$

$$xx; xx; xx = -xx; xy; xy = 3/2, yy; yy; yy = -yy; yx; yx = 3/2$$

$$\sigma^{x;xx} = -\sigma^{x;yy} = -\sigma_I^{y;yx} = -\sigma_{II}^{y;yx}, \sigma^{y;yy} = -\sigma^{y;xx} = -\sigma_I^{x;xy} = -\sigma_{II}^{x;xy}$$

- $G = 174 [\Gamma_h]$

$$U = \begin{pmatrix} 1 & 0 & 0 \\ 0 & 0 & -1 \\ 0 & 0 & 1 \\ 1 & 2 & 0 \\ -1 & 1 & 0 \\ -1 & -1 & 0 \\ 0 & -1 & 0 \\ -2 & -1 & 0 \end{pmatrix}, u = \begin{pmatrix} 0 \\ 0 \\ 1/2 \\ 1 \\ 1 \\ 0 \\ 0 \\ 1 \end{pmatrix}$$

- $F = D_6 (c_{6,z}, c_{2,x})$

$$xx; yy; zz = -xy; yx; zz = 6$$

$$\sigma^{x;yz} = -\sigma^{y;zx}, \text{Im } \sigma_I^{z;xy}$$

- $G = 177 - 182 [\Gamma_h]$

$$U = \begin{pmatrix} 1 & 0 & 0 \\ 0 & 0 & -1 \\ 0 & 0 & -1 \\ 0 & 0 & 1 \\ 1 & 2 & 0 \\ -2 & -1 & 0 \end{pmatrix}, u = \begin{pmatrix} 0 \\ 1/2 \\ 0 \\ 1/2 \\ 1 \\ 0 \end{pmatrix}$$

- $F = C_{6v} (c_{6,z}, \sigma_x)$

$$zz; zz; zz = 12, zz; xx; xx = zz; yy; yy = zz; xy; xy = 6,$$

$$\sigma^{z;zz}, \sigma^{z;xx} = \sigma^{z;yy}, \sigma^{x;xz} = \sigma^{y;yz}$$

- $G = 183 - 186 [\Gamma_h] \rightarrow$ Same as $G = 177$

- $F = D_{3h} (s_{3,z}, c_{2,x})$

$$xx; xx; xx = -xx; xy; xy = 3,$$

$$\sigma^{x;xx} = -\sigma^{x;yy} = -\sigma_I^{y;yx} = -\sigma_{II}^{y;yx}$$

- $G = 187 - 190 [\Gamma_h]$

$$U = \begin{pmatrix} 1 & 0 & 0 \\ 0 & 0 & -1 \\ 0 & 0 & 1 \\ 1 & 2 & 0 \\ -2 & -1 & 0 \\ -1 & 1 & 0 \\ -1 & -1 & 0 \end{pmatrix}, u = \begin{pmatrix} 0 \\ 0 \\ 1/2 \\ 1 \\ 0 \\ 1 \\ 0 \end{pmatrix}$$

- $F = T$

$$xx; yy; zz = xz; yx; zy = 4$$

$$\sigma^{x;yz} = \sigma^{y;zx} = \sigma^{z;xy}$$

- $G = 195 \text{ \& } 198 [\Gamma_c]$

$$\begin{pmatrix} \mathbf{G}_1^{\text{ref}} \\ \mathbf{G}_2^{\text{ref}} \\ \mathbf{G}_3^{\text{ref}} \end{pmatrix} = \begin{pmatrix} 1/a & 0 & 0 \\ 0 & 1/a & 0 \\ 0 & 0 & 1/a \end{pmatrix}, U = \begin{pmatrix} 0 & 1 & 0 \\ -1 & 0 & 1 \\ 0 & 0 & -1 \\ 0 & -1 & 1 \\ 1 & 0 & 0 \\ 0 & -1 & -1 \\ -1 & 0 & -1 \end{pmatrix}, u = \begin{pmatrix} 1/2 \\ 0 \\ 0 \\ 0 \\ 1/2 \\ 0 \\ 0 \end{pmatrix}$$

◦ $G = 196$ [Γ_c^f]

$$\begin{pmatrix} \mathbf{G}_1^{\text{ref}} \\ \mathbf{G}_2^{\text{ref}} \\ \mathbf{G}_3^{\text{ref}} \end{pmatrix} = \begin{pmatrix} -1/a & 1/a & 1/a \\ 1/a & -1/a & 1/a \\ 1/a & 1/a & -1/a \end{pmatrix}, U = \begin{pmatrix} 1 & 1 & 1 \\ 1 & -1 & 1 \\ -1 & -1 & 1 \\ 1 & 0 & -1 \\ -1 & 1 & 1 \\ 0 & 1 & -1 \\ -1 & -1 & 3 \\ 0 & -1 & 0 \\ -1 & 0 & 0 \end{pmatrix}, u = \begin{pmatrix} 3/2 \\ 1 \\ 0 \\ 1 \\ 0 \\ 3/2 \\ 0 \\ 0 \end{pmatrix}$$

◦ $G = 197$ & 199 [Γ_c^v]

$$\begin{pmatrix} \mathbf{G}_1^{\text{ref}} \\ \mathbf{G}_2^{\text{ref}} \\ \mathbf{G}_3^{\text{ref}} \end{pmatrix} = \begin{pmatrix} 0 & 1/a & 1/a \\ 1/a & 0 & 1/a \\ 1/a & 1/a & 0 \end{pmatrix}, U = \begin{pmatrix} 1 & 1 & 2 \\ 1 & 0 & -1 \\ -1 & -1 & 0 \\ 0 & 1 & -1 \\ -1 & -2 & -1 \\ -2 & -1 & -1 \end{pmatrix}, u = \begin{pmatrix} 1 \\ 0 \\ 0 \\ 0 \\ 0 \\ 0 \end{pmatrix}$$

• $F = O$

$$xx; yy; zz = xz; yx; zy = -xy; yx; zz = -xx; yz; zy = -xz; yy; zx = 4$$

$$\text{Im } \sigma_I^{x;yz} = \text{Im } \sigma_I^{y;zx} = \text{Im } \sigma_I^{z;xy}$$

◦ $G = 207 - 208$ & $212 - 213$ [Γ_c]

$$U = \begin{pmatrix} 1 & -1 & 0 \\ 0 & 1 & 0 \\ -1 & 0 & 1 \\ 0 & 0 & -1 \\ -1 & 0 & -1 \end{pmatrix}, u = \begin{pmatrix} 0 \\ 1/2 \\ 0 \\ 0 \\ 0 \end{pmatrix}$$

◦ $G = 209 - 210 [\Gamma_c^f]$

$$U = \begin{pmatrix} -1 & 1 & 0 \\ 1 & 1 & 1 \\ 1 & -1 & 1 \\ -1 & -1 & 1 \\ 1 & 0 & -1 \\ -1 & -1 & 3 \\ 0 & -1 & 0 \end{pmatrix}, \quad u = \begin{pmatrix} 0 \\ 3/2 \\ 1 \\ 0 \\ 0 \\ 3/2 \\ 0 \end{pmatrix}$$

◦ $G = 211 \text{ \& } 214 [\Gamma_c^v]$

$$U = \begin{pmatrix} -1 & 1 & 0 \\ 1 & 1 & 2 \\ 1 & 0 & -1 \\ -1 & -1 & 0 \\ -1 & -2 & -1 \end{pmatrix}, \quad u = \begin{pmatrix} 0 \\ 1 \\ 0 \\ 0 \\ 0 \end{pmatrix}$$

• $F = T_d$

$$xx; yy; zz = xz; yx; zy = xy; yx; zz = xx; yz; zy = xz; yy; zx = 4$$

$$\sigma_I^{x;yz} = \sigma_{II}^{x;yz} = \sigma_I^{y;zx} = \sigma_{II}^{y;zx} = \sigma_I^{z;xy} = \sigma_{II}^{z;xy}$$

◦ $G = 215 \text{ \& } 218 [\Gamma_c] \rightarrow$ Same as $G = 207$

◦ $G = 216 \text{ \& } 219 [\Gamma_c^f] \rightarrow$ Same as $G = 209$

◦ $G = 217 \text{ \& } 220 [\Gamma_c^v] \rightarrow$ Same as $G = 211$

The folded equation for magnetic point groups of type III, (20), can be readily computed from the previous list. Since the evaluation is slightly more involved, we next provide the explicit expressions for all non-vanishing components $\sigma_{\text{shift}}^{a;bc}$ in the non-trivial cases, namely for those groups M where H is non-centrosymmetric ($i \in H \Rightarrow \sigma_{\text{shift}}^{a;bc} = 0$) or there is \mathcal{PT} symmetry ($i \in F - H \Rightarrow \mathbb{D}^F = 0$), in which case (20) reduces to

$$\sigma_{\text{shift}}^{a;bc} = -\frac{i}{|H|N_{\mathbf{k}}^{\text{IBZ}}} \sum_{\mathbf{k} \in \text{IBZ}} \sum_{a',b',c'} \mathbb{D}_{a,a';b,b';c,c'}^H \text{Re} \left(\tilde{\sigma}_{\text{shift}}^{a';b'c'}(\mathbf{k}) - \tilde{\sigma}_{\text{shift}}^{a';c'b'}(\mathbf{k}) \right)$$

which can be evaluated straightforwardly as (18) or (19). The general form of the shift conductivity tensor can then be immediately identified from these expressions for any magnetic point group. The type III groups are labelled with an arbitrary number and in the Shubnikov-Belov notation as in Reference.⁵⁵ The orientation of each ordinary point group H and F is as in the previous list, except when specified by new generators. For simplicity, we omit the “shift” label, the \mathbf{k} dependence and the ubiquitous $\frac{1}{N_{\mathbf{k}}^{\text{IBZ}}} \sum_{\mathbf{k} \in \text{IBZ}}$ in the notation of the conductivity. The general relations $\sigma_{\text{shift}}^{a;bc} = (\sigma_{\text{shift}}^{a;cb})^*$ are also omitted.

-
- $M = 2$ ($2'$), $H = C_1$, $F = C_2$

$$\sigma^{a;bc} = \begin{cases} \text{Im} [\tilde{\sigma}^{a;bc} + \tilde{\sigma}^{a;cb}], & \text{if } \#x + \#y \text{ is even} \\ -i \text{Re} [\tilde{\sigma}^{a;bc} - \tilde{\sigma}^{a;cb}], & \text{if } \#x + \#y \text{ is odd} \end{cases}$$

where $\#x$ ($\#y$) is the number of times that x (y , resp.) appears in the (a, b, c) triplet.

- $M = 3$ (m'), $H = C_1$, $F = C_s$

$$\sigma^{a;bc} = \begin{cases} \text{Im} [\tilde{\sigma}^{a;bc} + \tilde{\sigma}^{a;cb}], & \text{if } \#x + \#y \text{ is odd} \\ -i \text{Re} [\tilde{\sigma}^{a;bc} - \tilde{\sigma}^{a;cb}], & \text{if } \#x + \#y \text{ is even} \end{cases}$$

where $\#x$ ($\#y$) is the number of times that x (y , resp.) appears in the (a, b, c) triplet.

- $M = 7$ ($2'2'2$), $H = C_2$, $F = D_2$

$$\begin{aligned} \sigma^{x;xz} &= -i \text{Re} [\tilde{\sigma}^{x;xz} - \tilde{\sigma}^{x;zx}], \quad \sigma^{y;yz} = -i \text{Re} [\tilde{\sigma}^{y;yz} - \tilde{\sigma}^{y;zy}], \\ \sigma^{x;yz} &= \text{Im} [\tilde{\sigma}^{x;yz} + \tilde{\sigma}^{x;zy}], \quad \sigma^{y;zx} = \text{Im} [\tilde{\sigma}^{y;zx} + \tilde{\sigma}^{y;xz}], \quad \sigma^{z;xy} = \text{Im} [\tilde{\sigma}^{z;xy} + \tilde{\sigma}^{z;yx}] \end{aligned}$$

- $M = 8$ ($m'm'2$), $H = C_2$, $F = C_{2v}$

$$\begin{aligned} \sigma^{z;zz} &= 2 \text{Im} \tilde{\sigma}^{z;zz}, \quad \sigma^{z;xx} = 2 \text{Im} \tilde{\sigma}^{z;xx}, \quad \sigma^{z;yy} = 2 \text{Im} \tilde{\sigma}^{z;yy}, \\ \sigma^{x;xz} &= \text{Im} [\tilde{\sigma}^{x;xz} + \tilde{\sigma}^{x;zx}], \quad \sigma^{y;yz} = \text{Im} [\tilde{\sigma}^{y;yz} + \tilde{\sigma}^{y;zy}], \quad \sigma^{x;yz} = -i \text{Re} [\tilde{\sigma}^{x;yz} - \tilde{\sigma}^{x;zy}], \\ \sigma^{y;zx} &= -i \text{Re} [\tilde{\sigma}^{y;zx} - \tilde{\sigma}^{y;xz}], \quad \sigma^{z;xy} = -i \text{Re} [\tilde{\sigma}^{z;xy} - \tilde{\sigma}^{z;yx}] \end{aligned}$$

- $M = 9$ ($m'm2'$), $H = C_s$ (σ_y), $F = C_{2v}$

$$\begin{aligned}\sigma^{z;zz} &= 2 \operatorname{Im} \tilde{\sigma}^{z;zz}, \quad \sigma^{z;xx} = 2 \operatorname{Im} \tilde{\sigma}^{z;xx}, \quad \sigma^{z;yy} = 2 \operatorname{Im} \tilde{\sigma}^{z;yy}, \quad \sigma^{y;yx} = -i \operatorname{Re} [\tilde{\sigma}^{y;yx} - \tilde{\sigma}^{y;xy}], \\ \sigma^{x;xz} &= \operatorname{Im} [\tilde{\sigma}^{x;xz} + \tilde{\sigma}^{x;zx}], \quad \sigma^{y;yz} = \operatorname{Im} [\tilde{\sigma}^{y;yz} + \tilde{\sigma}^{y;zy}], \quad \sigma^{z;zx} = -i \operatorname{Re} [\tilde{\sigma}^{z;zx} - \tilde{\sigma}^{z;xz}]\end{aligned}$$

- $M = 13$ ($4'$), $H = C_2$, $F = C_4$

$$\begin{aligned}\sigma^{z;zz} &= 2 \operatorname{Im} \tilde{\sigma}^{z;zz}, \quad \sigma^{z;xx} = \sigma^{z;yy} = \operatorname{Im} [\tilde{\sigma}^{z;xx} + \tilde{\sigma}^{z;yy}], \\ \sigma^{x;xz} &= (\sigma^{y;yz})^* = -\frac{i}{2} [\tilde{\sigma}^{x;xz} - (\tilde{\sigma}^{x;zx})^* - (\tilde{\sigma}^{y;yz})^* + \tilde{\sigma}^{y;zy}], \\ \sigma^{x;yz} &= -\sigma^{y;zx} = -\frac{i}{2} [\tilde{\sigma}^{x;yz} - (\tilde{\sigma}^{x;zy})^* + (\tilde{\sigma}^{y;xz})^* - \tilde{\sigma}^{y;zx}]\end{aligned}$$

- $M = 14$ ($\bar{4}'$), $H = C_2$, $F = S_4$

$$\begin{aligned}\sigma^{z;xx} &= -\sigma^{z;yy} = \operatorname{Im} [\tilde{\sigma}^{z;xx} - \tilde{\sigma}^{z;yy}], \quad \sigma^{x;xz} = -(\sigma^{y;yz})^* = -\frac{i}{2} [\tilde{\sigma}^{x;xz} - (\tilde{\sigma}^{x;zx})^* + (\tilde{\sigma}^{y;yz})^* - \tilde{\sigma}^{y;zy}], \\ \sigma^{x;yz} &= \sigma^{y;zx} = -\frac{i}{2} [\tilde{\sigma}^{x;yz} - (\tilde{\sigma}^{x;zy})^* - (\tilde{\sigma}^{y;xz})^* + \tilde{\sigma}^{y;zx}], \quad \sigma^{z;xy} = -i [\tilde{\sigma}^{z;xy} - (\tilde{\sigma}^{z;yx})^*]\end{aligned}$$

- $M = 15$ ($42'2'$), $H = C_4$, $F = D_4$

$$\begin{aligned}\sigma^{x;xz} &= \sigma^{y;yz} = -\frac{i}{2} \operatorname{Re} [\tilde{\sigma}^{x;xz} - \tilde{\sigma}^{x;zx} + \tilde{\sigma}^{y;yz} - \tilde{\sigma}^{y;zy}], \\ \sigma^{x;yz} &= -\sigma^{y;zx} = \frac{1}{2} \operatorname{Im} [\tilde{\sigma}^{x;yz} + \tilde{\sigma}^{x;zy} - \tilde{\sigma}^{y;xz} - \tilde{\sigma}^{y;zx}]\end{aligned}$$

- $M = 16$ ($4'22'$), $H = D_2$, $F = D_4$

$$\sigma^{x;yz} = -\sigma^{y;zx} = -\frac{i}{2} [\tilde{\sigma}^{x;yz} - (\tilde{\sigma}^{x;zy})^* + (\tilde{\sigma}^{y;xz})^* - \tilde{\sigma}^{y;zx}]$$

- $M = 20$ ($4m'm'$), $H = C_4$, $F = C_{4v}$

$$\begin{aligned}\sigma^{z;zz} &= 2 \operatorname{Im} \tilde{\sigma}^{z;zz}, \quad \sigma^{z;xx} = \sigma^{z;yy} = \operatorname{Im} [\tilde{\sigma}^{z;xx} + \tilde{\sigma}^{z;yy}], \\ \sigma^{x;xz} &= \sigma^{y;yz} = \frac{1}{2} \operatorname{Im} [\tilde{\sigma}^{x;xz} + \tilde{\sigma}^{x;zx} + \tilde{\sigma}^{y;yz} + \tilde{\sigma}^{y;zy}], \\ \sigma^{x;yz} &= \sigma^{y;zx} = -\frac{i}{2} \operatorname{Re} [\tilde{\sigma}^{x;yz} - \tilde{\sigma}^{x;zy} - \tilde{\sigma}^{y;xz} + \tilde{\sigma}^{y;zx}], \quad \sigma^{z;xy} = -i \operatorname{Re} [\tilde{\sigma}^{z;xy} - \tilde{\sigma}^{z;yx}]\end{aligned}$$

- $M = 21$ ($4'mm'$), $H = C_{2v}$, $F = C_{4v}$

$$\begin{aligned}\sigma^{z;zz} &= 2 \operatorname{Im} \tilde{\sigma}^{z;zz}, \quad \sigma^{z;xx} = \sigma^{z;yy} = \operatorname{Im} [\tilde{\sigma}^{z;xx} + \tilde{\sigma}^{z;yy}], \\ \sigma^{x;xz} &= (\sigma^{y;yz})^* = -\frac{i}{2} [\tilde{\sigma}^{x;xz} - (\tilde{\sigma}^{x;zx})^* - (\tilde{\sigma}^{y;yz})^* + \tilde{\sigma}^{y;zy}]\end{aligned}$$

- $M = 22$ ($\bar{4}2'm'$), $H = S_4$, $F = D_{2d}$

$$\begin{aligned}\sigma^{x;xz} &= -\sigma^{y;yz} = -\frac{i}{2} \operatorname{Re} [\tilde{\sigma}^{x;xz} - \tilde{\sigma}^{x;zx} - \tilde{\sigma}^{y;yz} + \tilde{\sigma}^{y;zy}], \\ \sigma^{x;yz} &= \sigma^{y;zx} = \frac{1}{2} \operatorname{Im} [\tilde{\sigma}^{x;yz} + \tilde{\sigma}^{x;zy} + \tilde{\sigma}^{y;xz} + \tilde{\sigma}^{y;zx}], \quad \sigma^{z;xy} = \operatorname{Im} [\tilde{\sigma}^{z;xy} + \tilde{\sigma}^{z;yx}]\end{aligned}$$

- $M = 23$ ($\bar{4}'2m'$), $H = D_2$, $F = D_{2d}$

$$\sigma^{x;yz} = \sigma^{y;zx} = -\frac{i}{2} [\tilde{\sigma}^{x;yz} - (\tilde{\sigma}^{x;zy})^* - (\tilde{\sigma}^{y;xz})^* + \tilde{\sigma}^{y;zx}], \quad \sigma^{z;xy} = -i [\tilde{\sigma}^{z;xy} - (\tilde{\sigma}^{z;yx})^*]$$

- $M = 24$ ($\bar{4}'m2'$), $H = C_{2v}$, $F = D_{2d}$ ($s_{4,z}$, σ_x)

$$\sigma^{z;xx} = -\sigma^{z;yy} = \operatorname{Im} [\tilde{\sigma}^{z;xx} - \tilde{\sigma}^{z;yy}], \quad \sigma^{x;xz} = -(\sigma^{y;yz})^* = -\frac{i}{2} [\tilde{\sigma}^{x;xz} - (\tilde{\sigma}^{x;zx})^* + (\tilde{\sigma}^{y;yz})^* - \tilde{\sigma}^{y;zy}]$$

- $M = 30$ ($32'$), $H = C_3$, $F = D_3$

$$\begin{aligned}\sigma^{x;xx} &= -\sigma^{x;yy} = -\sigma^{y;yx} = \frac{1}{2} \operatorname{Im} [\tilde{\sigma}^{x;xx} - \tilde{\sigma}^{x;yy} - \tilde{\sigma}^{y;yx} - \tilde{\sigma}^{y;xy}], \\ \sigma^{x;xz} &= \sigma^{y;yz} = -\frac{i}{2} \operatorname{Re} [\tilde{\sigma}^{x;xz} - \tilde{\sigma}^{x;zx} + \tilde{\sigma}^{y;yz} - \tilde{\sigma}^{y;zy}], \\ \sigma^{x;yz} &= -\sigma^{y;zx} = \frac{1}{2} \operatorname{Im} [\tilde{\sigma}^{x;yz} + \tilde{\sigma}^{x;zy} - \tilde{\sigma}^{y;zx} - \tilde{\sigma}^{y;zx}]\end{aligned}$$

- $M = 31$ ($3m'$), $H = C_3$, $F = C_{3v}$

$$\begin{aligned}\sigma^{x;xx} &= -\sigma^{x;yy} = -\sigma^{y;yx} = \frac{1}{2} \operatorname{Im} [\tilde{\sigma}^{x;xx} - \tilde{\sigma}^{x;yy} - \tilde{\sigma}^{y;yx} - \tilde{\sigma}^{y;xy}], \quad \sigma^{z;zz} = 2 \operatorname{Im} \tilde{\sigma}^{z;zz}, \\ \sigma^{z;xx} &= \sigma^{z;yy} = \operatorname{Im} [\tilde{\sigma}^{z;xx} + \tilde{\sigma}^{z;yy}], \quad \sigma^{x;xz} = \sigma^{y;yz} = \frac{1}{2} \operatorname{Im} [\tilde{\sigma}^{x;xz} + \tilde{\sigma}^{x;zx} + \tilde{\sigma}^{y;yz} + \tilde{\sigma}^{y;zy}], \\ \sigma^{x;yz} &= \sigma^{y;zx} = -\frac{i}{2} \operatorname{Re} [\tilde{\sigma}^{x;yz} - \tilde{\sigma}^{x;zy} - \tilde{\sigma}^{y;zx} + \tilde{\sigma}^{y;zx}], \quad \sigma^{z;xy} = -i \operatorname{Re} [\tilde{\sigma}^{z;xy} - \tilde{\sigma}^{z;yx}]\end{aligned}$$

- $M = 32$ ($\bar{6}'$), $H = C_3$, $F = C_{3h}$

$$\begin{aligned}\sigma^{x;xx} &= -\sigma^{x;yy} = -\sigma^{y;yx} = \frac{1}{2} \operatorname{Im} [\tilde{\sigma}^{x;xx} - \tilde{\sigma}^{x;yy} - \tilde{\sigma}^{y;yx} - \tilde{\sigma}^{y;xy}], \\ \sigma^{y;yy} &= -\sigma^{y;xx} = -\sigma^{x;xy} = \frac{1}{2} \operatorname{Im} [\tilde{\sigma}^{y;yy} - \tilde{\sigma}^{y;xx} - \tilde{\sigma}^{x;xy} - \tilde{\sigma}^{x;yx}], \\ \sigma^{x;xz} &= \sigma^{y;yz} = -\frac{i}{2} \operatorname{Re} [\tilde{\sigma}^{x;xz} - \tilde{\sigma}^{x;zx} + \tilde{\sigma}^{y;yz} - \tilde{\sigma}^{y;zy}], \\ \sigma^{x;yz} &= \sigma^{y;zx} = -\frac{i}{2} \operatorname{Re} [\tilde{\sigma}^{x;yz} - \tilde{\sigma}^{x;zy} - \tilde{\sigma}^{y;zx} + \tilde{\sigma}^{y;zx}], \quad \sigma^{z;xy} = -i \operatorname{Re} [\tilde{\sigma}^{z;xy} - \tilde{\sigma}^{z;yx}]\end{aligned}$$

- $M = 33$ ($\bar{6}m'2'$), $H = C_{3h}$, $F = D_{3h}$

$$\sigma^{x;xx} = -\sigma^{x;yy} = -\sigma^{y;yx} = \frac{1}{2} \operatorname{Im} [\tilde{\sigma}^{x;xx} - \tilde{\sigma}^{x;yy} - \tilde{\sigma}^{y;yx} - \tilde{\sigma}^{y;xy}]$$

- $M = 34$ ($\bar{6}'m2'$), $H = C_{3v}$, $F = D_{3h}$

$$\begin{aligned}\sigma^{x;xx} &= -\sigma^{x;yy} = -\sigma^{y;yx} = \frac{1}{2} \operatorname{Im} [\tilde{\sigma}^{x;xx} - \tilde{\sigma}^{x;yy} - \tilde{\sigma}^{y;yx} - \tilde{\sigma}^{y;xy}], \\ \sigma^{x;xz} &= \sigma^{y;yz} = -\frac{i}{2} \operatorname{Re} [\tilde{\sigma}^{x;xz} - \tilde{\sigma}^{x;zx} + \tilde{\sigma}^{y;yz} - \tilde{\sigma}^{y;zy}]\end{aligned}$$

- $M = 35 (\bar{6}'m'2)$, $H = D_3$, $F = D_{3h}$

$$\begin{aligned}\sigma^{x;xx} &= -\sigma^{x;yy} = -\sigma^{y;yx} = \frac{1}{2} \operatorname{Im} [\tilde{\sigma}^{x;xx} - \tilde{\sigma}^{x;yy} - \tilde{\sigma}^{y;yx} - \tilde{\sigma}^{y;xy}], \\ \sigma^{x;yz} &= \sigma^{y;zx} = -\frac{i}{2} \operatorname{Re} [\tilde{\sigma}^{x;yz} - \tilde{\sigma}^{x;zy} - \tilde{\sigma}^{y;xz} + \tilde{\sigma}^{y;zx}], \quad \sigma^{z;xy} = -i \operatorname{Re} [\tilde{\sigma}^{z;xy} - \tilde{\sigma}^{z;yx}]\end{aligned}$$

- $M = 36 (6')$, $H = C_3$, $F = C_6$

$$\begin{aligned}\sigma^{z;zz} &= 2 \operatorname{Im} \tilde{\sigma}^{z;zz}, \quad \sigma^{z;xx} = \sigma^{z;yy} = \operatorname{Im} [\tilde{\sigma}^{z;xx} + \tilde{\sigma}^{z;yy}], \\ \sigma^{x;xz} &= \sigma^{y;yz} = \frac{1}{2} \operatorname{Im} [\tilde{\sigma}^{x;xz} + \tilde{\sigma}^{x;zx} + \tilde{\sigma}^{y;yz} + \tilde{\sigma}^{y;zy}], \\ \sigma^{x;yz} &= -\sigma^{y;zx} = \frac{1}{2} \operatorname{Im} [\tilde{\sigma}^{x;yz} + \tilde{\sigma}^{x;zy} - \tilde{\sigma}^{y;xz} - \tilde{\sigma}^{y;zx}]\end{aligned}$$

- $M = 41 (62'2')$, $H = C_6$, $F = D_6$

$$\begin{aligned}\sigma^{x;xz} &= \sigma^{y;yz} = -\frac{i}{2} \operatorname{Re} [\tilde{\sigma}^{x;xz} - \tilde{\sigma}^{x;zx} + \tilde{\sigma}^{y;yz} - \tilde{\sigma}^{y;zy}], \\ \sigma^{x;yz} &= -\sigma^{y;zx} = \frac{1}{2} \operatorname{Im} [\tilde{\sigma}^{x;yz} + \tilde{\sigma}^{x;zy} - \tilde{\sigma}^{y;xz} - \tilde{\sigma}^{y;zx}]\end{aligned}$$

- $M = 42 (6'2'2)$, $H = D_3$, $F = D_6$

$$\sigma^{x;yz} = -\sigma^{y;zx} = \frac{1}{2} \operatorname{Im} [\tilde{\sigma}^{x;yz} + \tilde{\sigma}^{x;zy} - \tilde{\sigma}^{y;xz} - \tilde{\sigma}^{y;zx}]$$

- $M = 46 (6m'm')$, $H = C_6$, $F = C_{6v}$

$$\begin{aligned}\sigma^{z;zz} &= 2 \operatorname{Im} \tilde{\sigma}^{z;zz}, \quad \sigma^{z;xx} = \sigma^{z;yy} = \operatorname{Im} [\tilde{\sigma}^{z;xx} + \tilde{\sigma}^{z;yy}], \\ \sigma^{x;xz} &= \sigma^{y;yz} = \frac{1}{2} \operatorname{Im} [\tilde{\sigma}^{x;xz} + \tilde{\sigma}^{x;zx} + \tilde{\sigma}^{y;yz} + \tilde{\sigma}^{y;zy}], \\ \sigma^{x;yz} &= \sigma^{y;zx} = -\frac{i}{2} \operatorname{Re} [\tilde{\sigma}^{x;yz} - \tilde{\sigma}^{x;zy} - \tilde{\sigma}^{y;xz} + \tilde{\sigma}^{y;zx}], \quad \sigma^{z;xy} = -i \operatorname{Re} [\tilde{\sigma}^{z;xy} - \tilde{\sigma}^{z;yx}]\end{aligned}$$

- $M = 47$ ($6'm'm$), $H = C_{3v}$, $F = C_{6v}$

$$\begin{aligned}\sigma^{z;zz} &= 2 \operatorname{Im} \tilde{\sigma}^{z;zz}, \quad \sigma^{z;xx} = \sigma^{z;yy} = \operatorname{Im} [\tilde{\sigma}^{z;xx} + \tilde{\sigma}^{z;yy}], \\ \sigma^{x;xz} = \sigma^{y;yz} &= \frac{1}{2} \operatorname{Im} [\tilde{\sigma}^{x;xz} + \tilde{\sigma}^{x;zx} + \tilde{\sigma}^{y;yz} + \tilde{\sigma}^{y;zy}]\end{aligned}$$

- $M = 54$ ($\bar{4}3m'$), $H = T$, $F = T_d$

$$\sigma^{x;yz} = \sigma^{y;zx} = \sigma^{z;xy} = -\frac{i}{3} [\tilde{\sigma}^{x;yz} - (\tilde{\sigma}^{x;zy})^* + \tilde{\sigma}^{y;zx} - (\tilde{\sigma}^{y;xz})^* + \tilde{\sigma}^{z;xy} - (\tilde{\sigma}^{z;yx})^*]$$

- $M = 55$ ($4'32'$), $H = T$, $F = O$

$$\sigma^{a;bc} = 0, \quad \forall a, b, c$$

4 Conclusive remarks

The use of Gaussian basis sets to compute the shift conductivity has been proved satisfactory. The analytical evaluation of real-space integrals involving localized functions allows to readily compute the Berry connection and velocity matrix elements, while the reduced dimension yields lighter calculations, and the economical option of hybrid functionals allows to easily reproduce the desired band gap with good precision in a wide variety of systems. Furthermore, the (magnetic) space group symmetry is fully preserved and it can be capitalised on to perform maximally-efficient reciprocal space summations, in addition to immediately discerning the contributions to the electrical current under any light polarization.

The numerical results for the chosen materials are in standard agreement with the literature, and in all cases the length and velocity gauges have been shown to yield nearly identical outcomes. One would be tempted to conclude that the velocity gauge, in view of its comparative simplicity, should then be the preferred option in general. However, the length gauge makes no use of completeness relations and larger discrepancies may appear when

employing smaller bases. In addition, care should be taken when separating the shift and injection contributions without time-reversal symmetry in the velocity gauge. Nevertheless, the use of as-largest-as-possible basis sets is generally advisable, typically between TZVP and QZVP and including diffuse exponents. The use of ghost atoms, i.e., basis functions not located on atomic positions, could be explored in order to facilitate the reproduction of particularly-delocalized empty conduction states.

We note that all other single-particle contributions to the BPVE (in particular, the injection current) and to the total second-order optical response (in particular, the second-harmonic generation) can be computed from this method since the corresponding expressions involve the same basic quantities as the shift current. The transformation properties of these other optical contributions are the same for spatial operations, but the role of time-reversal may change. For example, the injection conductivity has the opposite behaviour to σ_{shift} , in the sense that time-reversal symmetry forces it to be imaginary (instead of real); and the results in Section 3 can be adapted from that. The evaluation of metallic systems is also possible in the length gauge, albeit it introduces additional terms with Fermi surface derivatives.³³

Supporting Information

Supporting Information available:

Input files for the self-consistent electronic structure calculations in CRYSTAL23 for each material (.d12 files, in the terminology of the code). Band structures along high-symmetry lines for each material. Explicit comparison between the BZ and IBZ summations in BaTiO₃.

Acknowledgement

The authors acknowledge financial support from Spanish MICINN (Grant Nos. PID2019-109539GB-C43 & TED2021-131323B-I00 & PID2022-141712NB-C21), María de Maeztu

Program for Units of Excellence in R&D (Grant No. CEX2018-000805-M), Comunidad Autónoma de Madrid through the Nanomag COST-CM Program (Grant No. S2018/NMT-4321), Generalitat Valenciana through Programa Prometeo (2021/017), Centro de Computación Científica of the Universidad Autónoma de Madrid, and Red Española de Supercomputación.

The authors declare no competing financial interest.

References

- (1) Sturman, B. I.; Fridkin, V. M. *The photovoltaic and photorefractive effects in noncentrosymmetric materials*; Gordon and Breach Science: Philadelphia, 1992.
- (2) Chynoweth, A. G. Surface space-charge layers in barium titanate. *Phys. Rev.* **1956**, *102*, 705–714.
- (3) Chen, F. S. Optically induced change of refractive indices in LiNbO₃ and LiTaO₃. *J. Appl. Phys.* **1969**, *40*, 3389–3396.
- (4) Glass, A. M.; Von der Linde, D.; Negran, T. J. High-voltage bulk photovoltaic effect and the photorefractive process in LiNbO₃. *Appl. Phys. Lett.* **1974**, *25*, 233–235.
- (5) Koch, W. T. H.; Munser, R.; Ruppel, W.; Würfel, P. Bulk photovoltaic effect in BaTiO₃. *Solid State Commun.* **1975**, *17*, 847–850.
- (6) Fridkin, V. M.; Popov, B. N.; Verkhovskaya, K. A. Effect of anomalous bulk photovoltage in ferroelectrics. *Phys. Status Solidi A* **1977**, *39*, 193–201.
- (7) Kraut, W.; von Baltz, R. Anomalous bulk photovoltaic effect in ferroelectrics: a quadratic response theory. *Phys. Rev. B* **1979**, *19*, 1548–1554.
- (8) von Baltz, R.; Kraut, W. Theory of the bulk photovoltaic effect in pure crystals. *Phys. Rev. B* **1981**, *23*, 5590–5596.

- (9) Hornung, D.; Von Baltz, R.; Rössler, U. Band structure investigation of the bulk photovoltaic effect in n-gap. *Solid State Commun.* **1983**, *48*, 225–229.
- (10) Fridkin, V.; Dalba, G.; Fornasini, P.; Soldo, Y.; Rocca, F.; Burattini, E. The bulk photovoltaic effect in LiNbO₃, crystals under x-ray synchrotron radiation. *Ferroelectrics Lett.* **1993**, *16*, 1–5.
- (11) Batirov, T.; Doubovik, E.; Djalalov, R.; Fridkin, V. M. The bulk photovoltaic effect in the piezoelectric crystal Pr₃Ga₅SiO₁₄. *Ferroelectrics Lett.* **1997**, *23*, 95–98.
- (12) Buse, K. Light-induced charge transport processes in photorefractive crystals II: materials. *Appl. Phys. B* **1997**, *64*, 391–407.
- (13) Král, P.; Mele, E. J.; Tománek, D. Photogalvanic effects in heteropolar nanotubes. *Phys. Rev. Lett.* **2000**, *85*, 1512–1515.
- (14) Sipe, J. E.; Shkrebtii, A. I. Second-order optical response in semiconductors. *Phys. Rev. B* **2000**, *61*, 5337–5352.
- (15) Butler, K. T.; Frost, J. M.; Walsh, A. Ferroelectric materials for solar energy conversion: photoferroics revisited. *Energ. Environ. Sci.* **2015**, *8*, 838–848.
- (16) Spanier, J. E.; Fridkin, V. M.; Rappe, A. M.; Akbashev, A. R.; Polemi, A.; Qi, Y.; Gu, Z.; Young, S. M.; Hawley, C. J.; Imbrenda, D., et al. Power conversion efficiency exceeding the Shockley-Queisser limit in a ferroelectric insulator. *Nat. Photonics* **2016**, *10*, 611–616.
- (17) Dai, Z.; Rappe, A. M. Recent progress in the theory of bulk photovoltaic effect. *Chem. Phys. Rev.* **2023**, *4*, 011303.1–26.
- (18) Cook, A. M.; Fregoso, B. M.; de Juan, F.; Coh, S.; Moore, J. E. Design principles for shift current photovoltaics. *Nat. Commun.* **2017**, *8*, 14176.1–9.

- (19) Rangel, T.; Fregoso, B. M.; Mendoza, B. S.; Morimoto, T.; Moore, J. E.; Neaton, J. B. Large bulk photovoltaic effect and spontaneous polarization of single-layer monochalcogenides. *Phys. Rev. Lett.* **2017**, *119*, 067402.1–6.
- (20) Osterhoudt, G. B.; Diebel, L. K.; Gray, M. J.; Yang, X.; Stanco, J.; Huang, X.; Shen, B.; Ni, N.; Moll, P. J. W.; Ran, Y., et al. Colossal mid-infrared bulk photovoltaic effect in a type-I Weyl semimetal. *Nat. Mater.* **2019**, *18*, 471–475.
- (21) Ahn, J.; Guo, G. Y.; Nagaosa, N. Low-frequency divergence and quantum geometry of the bulk photovoltaic effect in topological semimetals. *Phys. Rev. X* **2020**, *10*, 041041.1–28.
- (22) Wang, M.; Wei, H.; Wu, Y.; Jia, J.; Yang, C.; Chen, Y.; Chen, X.; Cao, B. Polarization-enhanced bulk photovoltaic effect of BiFeO₃ epitaxial film under standard solar illumination. *Phys. Lett. A* **2020**, *384*, 126831.1–6.
- (23) Xu, H.; Wang, H.; Zhou, J.; Li, J. Pure spin photocurrent in noncentrosymmetric crystals: bulk spin photovoltaic effect. *Nat. Commun.* **2021**, *12*, 4330.1–9.
- (24) Blázquez-Martínez, A.; Grysan, P.; Girod, S.; Glinsek, S.; Granzow, T. Direct evidence for bulk photovoltaic charge transport in a ferroelectric polycrystalline film. *Scripta Mater.* **2022**, *211*, 114498.1–5.
- (25) Chaudhary, S.; Lewandowski, C.; Refael, G. Shift-current response as a probe of quantum geometry and electron-electron interactions in twisted bilayer graphene. *Phys. Rev. Res.* **2022**, *4*, 013164.1–14.
- (26) Zhang, C.; Guo, P.; Zhou, J. Tailoring bulk photovoltaic effects in magnetic sliding ferroelectric materials. *Nano Lett.* **2022**, *22*, 9297–9305.
- (27) Dai, Z.; Schankler, A. M.; Gao, L.; Tan, L. Z.; Rappe, A. M. Phonon-assisted ballistic current from first-principles calculations. *Phys. Rev. Lett.* **2021**, *126*, 177403.1–6.

- (28) Xu, H.; Wang, H.; Li, J. Nonlinear nonreciprocal photocurrents under phonon dressing. *Phys. Rev. B* **2022**, *106*, 035102.1–7.
- (29) Dai, Z.; Rappe, A. M. First-principles calculation of ballistic current from electron-hole interaction. *Phys. Rev. B* **2021**, *104*, 235203.1–6.
- (30) Wang, H.; Tang, X.; Xu, H.; Li, J.; Qian, X. Generalized Wilson loop method for nonlinear light-matter interaction. *npj Quantum Mater.* **2022**, *7*, 61.1–7.
- (31) Parker, D. E.; Morimoto, T.; Orenstein, J.; Moore, J. E. Diagrammatic approach to nonlinear optical response with application to Weyl semimetals. *Phys. Rev. B* **2019**, *99*, 045121.1–20.
- (32) Ventura, G. B.; Passos, D. J.; Lopes Dos Santos, J. M. B.; Viana Parente Lopes, J. M.; Peres, N. M. R. Gauge covariances and nonlinear optical responses. *Phys. Rev. B* **2017**, *96*, 035431.1–11.
- (33) Taghizadeh, A.; Hipolito, F.; Pedersen, T. G. Linear and nonlinear optical response of crystals using length and velocity gauges: effect of basis truncation. *Phys. Rev. B* **2017**, *96*, 195413.1–10.
- (34) Passos, D. J.; Ventura, G. B.; Lopes, J. M., Viana Parente Lopes; Lopes dos Santos, J. M. B.; Peres, N. M. R. Nonlinear optical responses of crystalline systems: results from a velocity gauge analysis. *Phys. Rev. B* **2018**, *97*, 235446.1–11.
- (35) Young, S. M.; Rappe, A. M. First principles calculation of the shift current photovoltaic effect in ferroelectrics. *Phys. Rev. Lett.* **2012**, *109*, 116601.1–5.
- (36) Wang, C.; Liu, X.; Kang, L.; Gu, B. L.; Xu, Y.; Duan, W. First-principles calculation of nonlinear optical responses by Wannier interpolation. *Phys. Rev. B* **2017**, *96*, 115147.1–9.

- (37) Ibañez-Azpiroz, J.; Tsirkin, S. S.; Souza, I. Ab initio calculation of the shift photocurrent by Wannier interpolation. *Phys. Rev. B* **2018**, *97*, 245143.1–13.
- (38) Aversa, C.; Sipe, J. E. Nonlinear optical susceptibilities of semiconductors: results with a length-gauge analysis. *Phys. Rev. B* **1995**, *52*, 14636–14645.
- (39) Esteve-Paredes, J. J.; Palacios, J. J. A comprehensive study of the velocity, momentum and position matrix elements for Bloch states: application to a local orbital basis. *SciPost Phys. Core* **2023**, *6*, 002.1–20.
- (40) Doll, K.; Dovesi, R.; Orlando, R. Analytical Hartree-Fock gradients with respect to the cell parameter: systems periodic in one and two dimensions. *Theor. Chem. Acc.* **2006**, *115*, 354–360.
- (41) Dovesi, R.; Saunders, V. R.; Roetti, C.; Orlando, R.; Zicovich-Wilson, C. M.; Pascale, F.; Civalleri, B.; Doll, K.; Harrison, N. M.; Bush, I. J.; D’Arco, P.; Llunell, M.; Causà, M.; Noël, Y.; Maschio, L.; Erba, A.; Rerat, M.; Casassa, S. CRYSTAL17 user’s manual. <https://www.crystal.unito.it/include/manuals/crystal17.pdf>, Accessed on 07/2023.
- (42) Helgaker, T.; Jorgensen, P.; Olsen, J. *Molecular electronic-structure theory*; John Wiley & Sons: New York, 2013.
- (43) Gradshteyn, I. S.; M., R. I. *Table of integrals, series, and products*, seventh ed.; Elsevier: New York, 2007; Page 365, section 3.462, formula 2.
- (44) Bir, G. L.; Pikus, G. E. *Symmetry and strain-induced effects in semiconductors*; John Wiley & Sons: New York, 1974.
- (45) Dovesi, R.; Erba, A.; Orlando, R.; Zicovich-Wilson, C. M.; Civalleri, B.; Maschio, L.; Rerat, M.; Casassa, S.; Baima, J.; Salustro, S.; Kirtman, B. Quantum-mechanical

- condensed matter simulations with CRYSTAL. *WIREs Comput. Mol. Sci.* **2018**, *8*, e1360.1–36.
- (46) Erba, A.; Desmarais, J. K.; Casassa, S.; Civalleri, B.; Donà, L.; Bush, I. J.; Searle, B.; Maschio, L.; Daga, L.-E.; Cossard, A.; Ribaldone, C.; Ascrizzi, E.; Marana, N. L.; Flament, J.-P.; Kirtman, B.; Dovesi, R.; Erba, A.; Orlando, R.; Zicovich-Wilson, C. M.; Civalleri, B.; Maschio, L.; Rerat, M.; Casassa, S.; Baima, J.; Salustro, S.; Kirtman, B. CRYSTAL23: a program for computational solid state physics and chemistry. *J. Chem. Theory Comput.* **2022**,
- (47) Pritchard, B. P.; Altarawy, D.; Didier, B.; Gibson, T. D.; Windus, T. L. New basis set exchange: an open, up-to-date resource for the molecular sciences community. *J. Chem. Inf. Model.* **2019**, *59*, 4814–4820.
- (48) Laun, J.; Bredow, T. BSSE-corrected consistent Gaussian basis sets of triple-zeta valence with polarization quality of the fifth period for solid-state calculations. *J. Comput. Chem.* **2022**, *43*, 839–846.
- (49) Heyd, J.; Peralta, J. E.; Scuseria, G. E.; Martin, R. L. Energy band gaps and lattice parameters evaluated with the Heyd-Scuseria-Ernzerhof screened hybrid functional. *J. Chem. Phys.* **2005**, *123*, 174101.1–8.
- (50) Laun, J.; Bredow, T. BSSE-corrected consistent Gaussian basis sets of triple-zeta valence with polarization quality of the sixth period for solid-state calculations. *J. Comput. Chem.* **2021**, *42*, 1064–1072.
- (51) Perdew, J. P.; Burke, K.; Ernzerhof, M. Generalized gradient approximation made simple. *Phys. Rev. Lett.* **1996**, *77*, 3865.1–4.
- (52) Krukau, A. V.; Vydrov, O. A.; Izmaylov, A. F.; Scuseria, G. E. Influence of the exchange screening parameter on the performance of screened hybrid functionals. *J. Chem. Phys.* **2006**, *125*, 224106.1–5.

- (53) Gjerding, M. N.; Taghizadeh, A.; Rasmussen, A.; Ali, S.; Bertoldo, F.; Deilmann, T.; Knøsgaard, N. R.; Kruse, M.; Larsen, A. H.; Manti, S., et al. Recent progress of the computational 2D materials database (C2DB). *2D Mater.* **2021**, *8*, 044002.1–27.
- (54) Schankler, A. M.; Gao, L.; Rappe, A. M. Large bulk piezophotovoltaic effect of monolayer 2H-MoS₂. *J. Phys. Chem. Lett.* **2021**, *12*, 1244–1249.
- (55) Bradley, C.; Cracknell, A. *The mathematical theory of symmetry in solids: representation theory for point groups and space groups*; Oxford University Press: Oxford, 2010.

TOC Graphic

